

# The Inverse Gamma-Gamma Prior for Optimal Posterior Contraction and Multiple Hypothesis Testing <sup>\*</sup>

Ray Bai  
Malay Ghosh <sup>†</sup>

University of Florida

June 7, 2022

## Abstract

We study the well-known problem of estimating a sparse  $n$ -dimensional unknown mean vector  $\boldsymbol{\theta} = (\theta_1, \dots, \theta_n)$  with entries corrupted by Gaussian white noise. In the Bayesian framework, continuous shrinkage priors which can be expressed as scale-mixture normal densities are popular for obtaining sparse estimates of  $\boldsymbol{\theta}$ . In this article, we introduce a new fully Bayesian scale-mixture prior known as the inverse gamma-gamma (IGG) prior. We prove that the posterior distribution contracts around the true  $\boldsymbol{\theta}$  at (near) minimax rate under very mild conditions. In the process, we prove that the sufficient conditions for minimax posterior contraction given by van der Pas et al. [25] are not necessary for optimal posterior contraction. We further show that the IGG posterior density concentrates at a rate faster than those of the horseshoe or the horseshoe+ in the Kullback-Leibler (K-L) sense. To classify true signals ( $\theta_i \neq 0$ ), we also propose a hypothesis test based on thresholding the posterior mean. Taking the loss function to be the expected number of misclassified tests, we show that our test procedure asymptotically attains the optimal Bayes risk exactly. We illustrate through simulations and data analysis that the IGG has excellent finite sample performance for both estimation and classification.

---

<sup>\*</sup>Keywords and phrases: normal means problem, sparsity, nearly black vectors, posterior contraction, multiple hypothesis testing, heavy tail, shrinkage estimation

<sup>†</sup>Malay Ghosh (email: ghoshm@ufl.edu) is Distinguished Professor, Department of Statistics, University of Florida. Ray Bai (email: raybai07@ufl.edu) is Graduate Student, Department of Statistics, University of Florida.

# 1 Introduction

## 1.1 The Normal Means Problem Revisited

Suppose we observe an  $n$ -component random observation  $(X_1, \dots, X_n) \in \mathbb{R}^n$ , such that

$$X_i = \theta_i + \epsilon_i, \quad i = 1, \dots, n, \quad (1)$$

where  $\epsilon_i \sim N(0, 1), i = 1, \dots, n$ . In the high-dimensional setting where  $n$  is very large, sparsity is a very common phenomenon. That is, in the unknown mean vector  $\boldsymbol{\theta} = (\theta_1, \dots, \theta_n)$ , only a few of the  $\theta_i$ 's are nonzero. Under model (1), we are primarily interested in separating the signals ( $\theta_i \neq 0$ ) from the noise ( $\theta_i = 0$ ) and giving robust estimates of the signals.

This simple framework (1) is the basis for a number of high-dimensional problems, such as image reconstruction, genetics, and wavelet analysis (Johnstone and Silverman [20]). For example, if we wish to reconstruct an image from millions of pixels of data, only a few pixels are typically needed to recover the objects of interest. In genetics, we may have tens of thousands of gene expression data points, but only a few are significantly associated with the phenotype of interest. For instance, Wellcome Trust [28] has confirmed that only seven genes have a non-negligible association with Type I diabetes. These applications demonstrate that sparsity is a fairly reasonable assumption for  $\boldsymbol{\theta}$  in (1).

## 1.2 Scale-Mixture Shrinkage Priors

Scale-mixture shrinkage priors are widely used for obtaining sparse estimates of  $\boldsymbol{\theta}$  in (1). These priors typically take the form

$$\theta_i | \sigma_i^2 \sim N(0, \sigma_i^2), \quad \sigma_i^2 \sim \pi(\sigma_i^2), \quad i = 1, \dots, n, \quad (2)$$

where  $\pi : [0, \infty) \rightarrow [0, \infty)$  is a density on the positive reals. These scale-mixture densities typically contain heavy mass around zero, so that the posterior density is heavily concentrated around  $\mathbf{0} \in \mathbb{R}^n$ . However, they also retain heavy enough tails in order to correctly identify and prevent overshrinkage of the true signals.

Global-local (GL) shrinkage priors comprise a wide class of scale-mixture shrinkage priors (2). GL priors take the form

$$\theta_i | \tau, \lambda_i \sim N(0, \lambda_i \tau), \quad \lambda_i \sim f, \quad \tau \sim g, \quad (3)$$

where  $\tau$  is a global shrinkage parameter that shrinks all  $\theta_i$ 's to the origin, while the local scale parameters  $\lambda_i$ 's control the degree of individual shrinkage. Examples of GL priors include the Bayesian lasso (Park and Casella

[21]), the horseshoe prior (Carvalho et al. [9]), the Strawderman-Berger prior (Strawderman [24], Berger [4]), the normal-exponential-gamma (NEG) prior (Griffin and Brown [19]), the Dirichlet-Laplace prior (Bhattacharya et al. [6]), the generalized double Pareto (GDP) family (Armagan et al. [2]), and the horseshoe+ prior (Bhadra et al. [5]).

The three parameter beta normal (TPBN) mixture family introduced by Armagan et al. [1] generalizes several well-known scale-mixture shrinkage priors. The TPBN family places a beta prime density (also known as the inverted beta) as the prior on  $\lambda_i$  in (3), i.e.

$$\pi(\lambda_i) = \frac{\Gamma(a+b)}{\Gamma(a)\Gamma(b)} \lambda_i^{a-1} (1+\lambda_i)^{-(a+b)}, i = 1, \dots, n, \quad (4)$$

where  $a$  and  $b$  are positive constants. Examples of priors that fall under the TPBN family include the horseshoe prior ( $a = b = 0.5$ ), the Strawderman-Berger prior ( $a = 1, b = 0.5$ ), and the normal-exponential gamma (NEG) prior ( $a = 1, b > 0$ ).

GL priors have been studied extensively in the context of sparse normal means estimation. Many authors have shown that the posterior distribution under GL priors contracts at (near) minimax rate. Most of the past posterior contraction results have relied on tuning or estimating the global parameter  $\tau$  to achieve this rate. The  $\tau$  in (3) can either be a priori specified with a specific rate of decay (as in van der Pas et al. [27] or Ghosh and Chakrabarti [16]) or it can be estimated from the data through empirical Bayes or by placing a prior on  $\tau$  (as in van der Pas et al. [27], van der Pas et al. [26], and Bhattacharya et al. [6]).

Moving beyond the global-local framework, van der Pas et al. [25] provided conditions for which the posterior distribution under *any* scale-mixture shrinkage prior of the form (2) achieves the minimax posterior contraction rate, provided that the  $\theta_i$ 's are *a posteriori* independent. Their result is quite general and covers a wide variety of priors, including the normal-gamma prior (Griffin and Brown [18]), the spike-and-slab LASSO (Ročková [22]) and the horseshoe+ prior (Bhadra et al. [5]). A thorough discussion of optimal posterior contraction is given in Section 3.

In addition to robust estimation of  $\boldsymbol{\theta}$ , we are often interested in identifying the true signals (or non-zero entries) within  $\boldsymbol{\theta}$ . Here, we are essentially conducting  $n$  simultaneous hypothesis tests,  $H_{0i}$ :  $\theta_i = 0$  vs.  $H_{1i}$ :  $\theta_i \neq 0, i = 1, \dots, n$ . Assuming that the true data-generating model is a two-components mixture density, Bogdan et al. [7] studied the risk properties of a large number of multiple testing rules. Specifically, Bogdan et al.

[7] considered a symmetric 0-1 loss function taken to be the expected total number of misclassified tests. By imposing a few regularity conditions to induce sparsity and to bound the Type I and Type II error probabilities away from zero and one, Bogdan et al. [7] arrived at a simple closed form for the asymptotic Bayes risk under 0-1 loss. They termed this as the asymptotically Bayes optimal risk under sparsity (or ABOS risk). They then provided necessary and sufficient conditions for which a number of classical multiple test procedures (e.g. the Benjamini and Hochberg [3] procedure) could asymptotically match the ABOS risk, provided that the true  $\theta_i$ 's are generated from a point mass-mixture density. A thorough discussion of this decision theoretic framework is presented in Section 4.1.

Testing rules induced by scale-mixture shrinkage priors – specifically GL priors (3) – have also been studied in this decision theoretic framework. Assuming that the  $\theta_i$ 's come from a two-components model, Datta and Ghosh [12] showed that a thresholding rule based on the posterior mean under the horseshoe prior could asymptotically attain the ABOS risk up to a multiplicative constant. Ghosh et al. [17] generalized this result to a general class of shrinkage priors of the form (3), including the student-t distribution, the TPBN family, and the GDP family of priors. Ghosh and Chakrabarti [16] later showed that their thresholding rule for this same class of priors could even asymptotically attain the ABOS risk exactly. Bhadra et al. [5] also extended this same rule for the horseshoe+ prior, showing that a testing rule based on the horseshoe+ prior could asymptotically attain the ABOS risk up to a multiplicative constant. In all of the aforementioned papers, the global parameter  $\tau$  in (3) was treated as either a tuning parameter that decays to zero as  $n \rightarrow \infty$  or set as a plug-in empirical Bayes estimate  $\hat{\tau}$  from van der Pas et al. [27].

In this article, we introduce a new fully Bayesian scale-mixture shrinkage prior. Our goal is twofold. Having observed a vector  $\mathbf{X} = (X_1, \dots, X_n)$  with entries from (1), we would like to achieve: 1) robust estimation of  $\boldsymbol{\theta}$ , and 2) a robust testing rule for identifying true signals. To tackle both these problems, we introduce a new scale-mixture shrinkage prior known as the Inverse Gamma-Gamma (IGG) prior.

The IGG prior has a number of attractive theoretical properties. Under extremely mild conditions and with specification of appropriate hyperparameters, the IGG posterior density is able to attain the (near) minimax contraction rate. Our work differs from the existing literature in several notable ways. First, the IGG is a special case of the TPBN prior density (4). However, we show that we can achieve (near) minimax posterior contraction by simply specifying sample-size dependent hyperparameters  $a$  and

$b$ , rather than by tuning or estimating a shared global parameter  $\tau$ . Our prior therefore does not fall under the global-local framework and our theoretical results differ from many existing results based on global-local priors. Moreover, our prior is an example of a scale-mixture shrinkage prior that does *not* necessarily satisfy the conditions for optimal contraction given by van der Pas et al. [25], thus proving that these conditions are not necessary for minimax-optimal posterior contraction. Finally, we justify the use of the IGG by showing that the posterior concentrates at a rate faster than any known Bayes estimator (including the horseshoe and horseshoe+ densities) in the Kullback-Leibler sense.

In addition, we show that our testing rule for classifying signals asymptotically achieves the optimal Bayes risk exactly. While previously, Ghosh and Chakrabarti [16] demonstrated that testing rules based on global-local priors could asymptotically attain the optimal Bayes risk exactly, their result required tuning or estimating a global parameter  $\tau$ . The IGG prior avoids this by placing appropriate values (dependent upon sample size) as its hyperparameters instead.

The organization of this paper is as follows. In Section 2, we introduce the IGG prior. We show that it mimics traditional shrinkage priors by placing heavy mass around zero. We also establish various concentration properties of the IGG prior that characterize its tail behavior and that are crucial for establishing our theoretical results. In Section 3, we discuss the behavior of the posterior under the IGG prior. We show that for a class of sparse normal mean vectors, the posterior distribution under the IGG prior contracts around the true  $\theta$  at (near) minimax rate under mild conditions, and moreover, that the posterior concentrates at a faster rate than any known Bayes estimator. In Section 4, we introduce our thresholding rule based on the posterior mean and demonstrate that it asymptotically attains the ABOS risk exactly. In Section 5, we present simulation results which demonstrate that the IGG prior has excellent performance for both estimation and classification in finite samples. Finally, in Section 6, we utilize the IGG prior to analyze a prostate cancer data set.

### 1.3 Notation

We use the following notations for the rest of the paper. Let  $\{a_n\}$  and  $\{b_n\}$  be two non-negative sequences of real numbers indexed by  $n$ , where  $b_n \neq 0$  for sufficiently large  $n$ . We write  $a_n \asymp b_n$  to denote  $0 < \liminf_{n \rightarrow \infty} \frac{a_n}{b_n} \leq \limsup_{n \rightarrow \infty} \frac{a_n}{b_n} < \infty$ , and  $a_n \lesssim b_n$  to denote that there exists a constant  $C > 0$

independent of  $n$  such that  $a_n \leq Cb_n$  provided  $n$  is sufficiently large. If  $\lim_{n \rightarrow \infty} \frac{a_n}{b_n} = 1$ , we write it as  $a_n \sim b_n$ . Moreover, if  $\left| \frac{a_n}{b_n} \right| \leq M$  for all sufficiently large  $n$  where  $M > 0$  is a positive constant independent of  $n$ , then we write  $a_n = O(b_n)$ . If  $\lim_{n \rightarrow \infty} \frac{a_n}{b_n} = 0$ , we write  $a_n = o(b_n)$ . Thus,  $a_n = o(1)$  if  $\lim_{n \rightarrow \infty} a_n = 0$ .

Throughout the paper, we also use  $Z$  to denote a standard normal  $N(0, 1)$  random variable having cumulative distribution function and probability density function  $\Phi(\cdot)$  and  $\phi(\cdot)$ , respectively.

## 2 The Inverse Gamma-Gamma (IGG) Prior

Suppose we have observed  $\mathbf{X} \sim \mathcal{N}(\boldsymbol{\theta}, \mathbf{I}_n)$ , and our task is to estimate the  $n$ -dimensional vector,  $\boldsymbol{\theta}$ . Consider putting a scale-mixture prior on each  $\theta_i, i = 1, \dots, n$  of the form

$$\begin{aligned} \theta_i | \sigma_i^2 &\overset{ind}{\sim} N(0, \sigma_i^2), i = 1, \dots, n, \\ \sigma_i^2 &\overset{i.i.d.}{\sim} \beta'(a, b), i = 1, \dots, n, \end{aligned} \quad (5)$$

where  $\beta'(a, b)$  denotes the beta prime density (4). The scale mixture prior (5) is a special case of the TPBN family of priors with the global parameter  $\tau$  fixed at  $\tau = 1$ . From (5), one easily sees that the posterior mean of  $\theta_i$  under (5) is given by

$$\mathbb{E}\{\mathbb{E}(\theta_i | X_i, \sigma^2)\} = \{\mathbb{E}(1 - \kappa_i) | X_i\} X_i, \quad (6)$$

where  $\kappa_i = \frac{1}{1 + \sigma_i^2}$ . Using a simple transformation of variables, we also see that the posterior density of the shrinkage factor  $\kappa_i$  is proportional to

$$\pi(\kappa_i | X_i) \exp\left(-\frac{\kappa_i X_i^2}{2}\right) \kappa_i^{a-1/2} (1 - \kappa_i)^{b-1}, \quad \kappa_i \in (0, 1). \quad (7)$$

From (6), it is clear that the amount of shrinkage is controlled by the shrinkage factor  $\kappa_i$ . With appropriately chosen  $a$  and  $b$ , one can obtain sparse estimates of the  $\theta_i$ 's. For example, with  $a = b = 0.5$ , we obtain the standard half-Cauchy density  $C^+(0, 1)$ .

To distinguish our work from previous results, we note that the beta prime density (4) can be rewritten as a product of independent inverse gamma and gamma densities. We reparametrize (5) as follows:

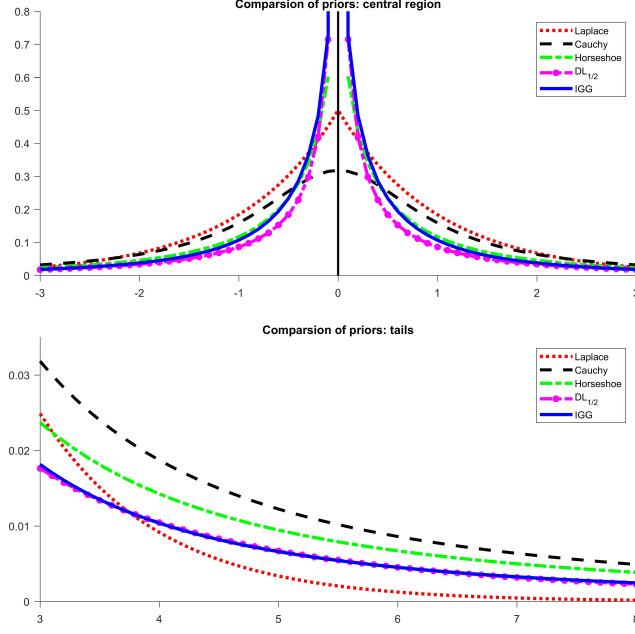


Figure 1: Marginal density of the IGG prior (8) with hyperparameters  $a = 0.6, b = 0.4$ , in comparison to other shrinkage priors. The  $DL_{1/2}$  prior is the marginal density for the Dirichlet-Laplace density with  $\text{Dir}(1/2, \dots, 1/2)$  specified as a prior in the Bayesian hierarchy.

$$\begin{aligned}
 \theta_i | \lambda_i, \xi_i &\stackrel{\text{ind}}{\sim} N(0, \lambda_i \xi_i), i = 1, \dots, n, \\
 \lambda_i &\stackrel{i.i.d.}{\sim} \mathcal{G}(a, 1), i = 1, \dots, n, \\
 \xi_i &\stackrel{i.i.d.}{\sim} \mathcal{IG}(b, 1), i = 1, \dots, n,
 \end{aligned} \tag{8}$$

where  $a, b > 0$ . It should be noted that the rate parameter 1 in (8) could be replaced by any positive constant. Representation (8) gives us some important intuition into the behavior of the IGG prior. Namely, for small values of  $b$ ,  $\mathcal{IG}(b, 1)$  places more mass around zero. As Proposition 1 shows, for any  $0 < b \leq \frac{1}{2}$ , the marginal distribution for a single  $\theta$  under the IGG prior has a singularity at zero.

**Proposition 1.** *If  $\theta$  is endowed with the IGG prior (8), then the marginal distribution of  $\theta$  is unbounded with a singularity at zero for any  $0 < b \leq 1/2$ .*

*Proof.* See Appendix A. □

Proposition 1 gives us some insight into how we should choose the hyperparameters in (8). Namely, we see that for small values of  $b$ , the IGG prior can induce sparse estimates of the  $\theta_i$ 's by shrinking most observations to zero. As we will illustrate in Section 2.1, the tails of the IGG prior are still heavy enough to identify signals that are significantly far away from zero.

Figure 1 gives a plot of the marginal density  $\pi(\theta_i)$  for the IGG prior (8), with  $a = 0.6$  and  $b = 0.4$ . Figure 1 shows that with a small value for  $b$ , the IGG has a singularity at zero. The IGG prior also appears to have slightly heavier mass around zero than other well-known scale-mixture shrinkage priors, but maintaining the same tail robustness. In Section 3, we provide a theoretical argument that shows that the shrinkage profile near zero under the IGG is indeed more aggressive than that of previous known Bayesian estimators.

## 2.1 Concentration Properties of the IGG Prior

Consider the IGG prior given in (8), but now we allow the hyperparameter  $b_n$  is allowed to vary with  $n$  as  $n \rightarrow \infty$ . Namely, we allow  $0 < b_n < 1$  for all  $n$ , but  $b_n \rightarrow 0$  as  $n \rightarrow \infty$  so that even more mass is placed around zero as  $n \rightarrow \infty$ . We also fix  $a$  to lie in the interval  $(\frac{1}{2}, \infty)$ . To emphasize that the hyperparameter  $b_n$  depends on  $n$ , we rewrite the prior (8) as

$$\begin{aligned}\theta_i | \lambda_i, \xi_i &\stackrel{i.i.d.}{\sim} N(0, \lambda_i \xi_i), i = 1, \dots, n, \\ \lambda_i &\stackrel{i.i.d.}{\sim} \mathcal{IG}(a, 1), i = 1, \dots, n, \\ \xi_i &\stackrel{i.i.d.}{\sim} \mathcal{G}(b_n, 1), i = 1, \dots, n,\end{aligned}\tag{9}$$

where  $b_n \in (0, 1) = o(1)$  and  $a \in (\frac{1}{2}, \infty)$ . For the rest of the paper, we label this particular variant of the IGG prior as the  $\text{IGG}_n$  prior.

As described in Section 2, the shrinkage factor  $\kappa_i = \frac{1}{1 + \lambda_i \xi_i}$  plays a critical role in the amount of shrinkage of each observation  $X_i$ . In this section, we further characterize the tail properties of the posterior distribution  $\pi(\kappa_i | X_i)$ , which demonstrates that the  $\text{IGG}_n$  prior (9) shrinks most estimates of  $\theta_i$ 's to zero but still has heavy enough tails to identify true signals. In the following results, we assume the  $\text{IGG}_n$  prior on  $\theta_i$  for  $X_i \sim N(\theta_i, 1)$ .

**Theorem 1.** *For any  $a, b_n \in (0, \infty)$ ,*

$$\mathbb{E}(1 - \kappa_i | X_i) \leq e^{X_i^2/2} \left( \frac{b_n}{a + b_n + 1/2} \right).$$

*Proof.* See Appendix A. □



**Corollary 1.1.** *If  $a$  is fixed and  $b_n \rightarrow 0$  as  $n \rightarrow \infty$ , then  $\mathbb{E}(1 - \kappa_i | X_i) \rightarrow 0$  as  $n \rightarrow \infty$ .*

**Theorem 2.** *Fix  $\epsilon \in (0, 1)$ . For any  $a \in (\frac{1}{2}, \infty)$ ,  $b_n \in (0, 1)$ ,*

$$P(\kappa_i < \epsilon | X_i) \leq e^{X_i^2/2} \frac{b_n \epsilon}{(a + 1/2)(1 - \epsilon)}.$$

*Proof.* See Appendix A. □

**Corollary 2.1.** *If  $a \in (\frac{1}{2}, \infty)$  is fixed and  $b_n \rightarrow 0$  as  $n \rightarrow \infty$ , then by Theorem 2,  $P(\kappa_i \geq \epsilon | X_i) \rightarrow 1$  for any fixed  $\epsilon \in (0, 1)$ .*

**Theorem 3.** *Fix  $\eta \in (0, 1)$ ,  $\delta \in (0, 1)$ . Then for any  $a \in (\frac{1}{2}, \infty)$  and  $b_n \in (0, 1)$ ,*

$$P(\kappa_i > \eta | X_i) \leq \frac{\left(a + \frac{1}{2}\right)(1 - \eta)^{b_n}}{b_n(\eta\delta)^{a+\frac{1}{2}}} \exp\left(-\frac{\eta(1 - \delta)}{2} X_i^2\right).$$

*Proof.* See Appendix A. □

**Corollary 3.1.** *For any fixed  $n$  where  $a \in (\frac{1}{2}, \infty)$ ,  $b_n \in (0, 1)$ , and for every fixed  $\eta \in (0, 1)$ ,  $P(\kappa_i \leq \eta | X_i) \rightarrow 1$  as  $X_i \rightarrow \infty$ .*

**Corollary 3.2.** *For any fixed  $n$  where  $a \in (\frac{1}{2}, \infty)$ ,  $b_n \in (0, 1)$ , and for every fixed  $\eta \in (0, 1)$ ,  $E(1 - \kappa_i | X_i) \rightarrow 1$  as  $X_i \rightarrow \infty$ .*

Since  $\mathbb{E}(\theta_i | X_i) = \{\mathbb{E}(1 - \kappa_i) | X_i\} X_i$ , Corollaries 1.1 and 2.1 illustrate that all observations will be shrunk towards the origin under the  $\text{IGG}_n$  prior (9). However, Corollaries 3.1 and 3.2 demonstrate that if  $X_i$  is big enough, then the posterior mean  $\{\mathbb{E}(1 - \kappa_i) | X_i\} X_i \approx X_i$ . This assures us that the tails of the  $\text{IGG}$  prior are still sufficiently heavy to detect true signals.

We will use the concentration properties established in Theorem 1 and 3 to provide sufficient conditions for which the posterior mean and posterior distribution under the  $\text{IGG}_n$  prior (9) contract around the true  $\theta_0$  at minimax or near-minimax rate in Section 3. These concentration properties will also help us to construct the multiple testing procedure based on  $\kappa_i$  in Section 4.

### 3 Posterior Behavior Under the IGG Prior

#### 3.1 Sparse Normal Vectors in the Nearly Black Sense

Suppose that we observe  $\mathbf{X} = (X_1, \dots, X_n) \in \mathbb{R}^n$  from (1). Let  $\ell_0[q_n]$  denote the subset of  $\mathbb{R}^n$  given by

$$\ell_0[q_n] = \{\boldsymbol{\theta} \in \mathbb{R}^n : \#(1 \leq j \leq n : \theta_j \neq 0) \leq q_n\}. \quad (10)$$

If  $\boldsymbol{\theta} \in \ell_0[q_n]$  with  $q_n = o(n)$  as  $n \rightarrow \infty$ , we say that  $\boldsymbol{\theta}$  is sparse in the “nearly black sense.” Let  $\boldsymbol{\theta}_0 = (\theta_{01}, \dots, \theta_{0n})$  be the true mean vector. In their seminal work, Donoho et al. [13] showed that for any estimator of  $\boldsymbol{\theta}$ , denoted by  $\hat{\boldsymbol{\theta}}$ , the corresponding minimax risk with respect to the  $l_2$ - norm is given by

$$\inf_{\hat{\boldsymbol{\theta}}} \sup_{\boldsymbol{\theta}_0 \in \ell_0[q_n]} \mathbb{E}_{\boldsymbol{\theta}_0} \|\hat{\boldsymbol{\theta}} - \boldsymbol{\theta}_0\|^2 = 2q_n \log\left(\frac{n}{q_n}\right) (1 + o(1)), \text{ as } n \rightarrow \infty. \quad (11)$$

In (11) and throughout the paper,  $\mathbb{E}_{\boldsymbol{\theta}_0}$  denotes expectation with respect to the  $\mathcal{N}(\boldsymbol{\theta}_0, \mathbf{I}_n)$  distribution. (11) effectively states that in the presence of sparsity, a minimax-optimal estimator only loses as a logarithmic factor (in the ambient dimension) as a penalty for not knowing the true locations of the zeroes. Moreover, (11) implies that we only need a number of replicates in the order of the true sparsity level  $q_n$  to consistently estimate  $\boldsymbol{\theta}_0$ . In order for the performance of Bayesian estimators to be compared with frequentist ones, we say that a Bayesian point estimator  $\hat{\boldsymbol{\theta}}^B$  attains the minimax risk (in the order of a constant) if

$$\sup_{\boldsymbol{\theta}_0 \in \ell_0[q_n]} \mathbb{E}_{\boldsymbol{\theta}_0} \|\hat{\boldsymbol{\theta}}^B - \boldsymbol{\theta}_0\|^2 \asymp q_n \log\left(\frac{n}{q_n}\right). \quad (12)$$

Examples of potential choices for  $\hat{\boldsymbol{\theta}}^B$  include the posterior median or the posterior mean (as in Johnstone and Silverman [20]), or the posterior mode (as in Ročková [22]). (12) pertains only to a particular point estimate. For a *fully* Bayesian interpretation, we say that the posterior distribution contracts around the true  $\boldsymbol{\theta}_0$  at a rate at least as fast as the minimax  $l_2$  risk if

$$\sup_{\boldsymbol{\theta}_0 \in \ell_0[q_n]} \mathbb{E}_{\boldsymbol{\theta}_0} \Pi\left(\boldsymbol{\theta} : \|\boldsymbol{\theta} - \boldsymbol{\theta}_0\|^2 > M_n q_n \log\left(\frac{n}{q_n}\right) \middle| \mathbf{X}\right) \rightarrow 0, \quad (13)$$

for every  $M_n \rightarrow \infty$  as  $n \rightarrow \infty$ . On the other hand, in another seminal paper, Ghosal et al. [15] showed that the posterior distribution cannot contract

faster than the minimax rate of  $q_n \log \left( \frac{n}{q_n} \right)$  around the truth. Hence, the optimal rate of contraction of a posterior distribution around the true  $\theta_0$  must be the minimax optimal rate in (11), up to some multiplicative constant. In other words, if we use a fully Bayesian model to estimate a “nearly black” normal mean vector, the minimax optimal rate should be our benchmark, and the posterior distribution should capture the true  $\theta_0$  in a ball of squared radius at most  $q_n \log \left( \frac{n}{q_n} \right)$  (up to a multiplicative constant) as  $n \rightarrow \infty$ .

In the subsequent section, we first prove that the  $\text{IGG}_n$  prior does not satisfy the conditions for posterior contraction given by van der Pas et al. [25] for scale-mixture shrinkage priors (2). We then provide sufficient conditions on the rate of decay of  $b_n$  in (9) such that, under the  $\text{IGG}_n$  prior, the posterior mean attains the minimax risk, while the posterior distribution contracts at the minimax rate. In order for (12) and (13) to hold for the  $\text{IGG}_n$  prior, the true sparsity level  $q_n$  must be known. However, if  $q_n$  is unknown, then the  $\text{IGG}_n$  prior can still attain near-minimax concentration rates.

### 3.2 Minimax Posterior Contraction Under the IGG Prior

For scale-mixture shrinkage priors (2) where the priors on  $\sigma_i^2$ 's,  $i = 1, \dots, n$ , are a priori independent, van der Pas et al. [25] gave sufficient conditions under which the posterior contracts at the minimax rate given in (13). A variety of densities  $\pi(\sigma_i^2)$  are known to satisfy these conditions, including the horseshoe and horseshoe+ priors, the spike-and-slab LASSO, the normal-gamma prior, and the inverse Gaussian prior. We first demonstrate that the IGG prior (9) prior can fail to satisfy these conditions before proceeding to provide conditions under which it *does* achieve the minimax posterior contraction rate. We first restate Theorem 2.1 from van der Pas et al. [25] below:

**Proposition 2** (Van der Pas et al., 2016). *Suppose that  $\mathbf{X} = (X_1, \dots, X_n) \sim \mathcal{N}(\theta_0, \mathbf{I}_n)$  is observed, and assume that the prior on  $\theta$  is of form (2). Suppose further that  $q_n = o(n)$  and let  $M_n$  be an arbitrary positive sequence tending to  $+\infty$ . Suppose that the following conditions on the scale prior  $\pi$  hold:*

1. *For some  $b \geq 0$ , we can write  $u \mapsto \pi(u) = L_n(u)e^{-bu}$ , where  $L_n$  is a function that is uniformly regular varying. That is, there exist constants  $R, u_0 \geq 1$  (which do not depend on  $n$ ), such that*

$$\frac{1}{R} \leq \frac{L(au)}{L(u)} \leq R, \text{ for all } a \in [1, 2], \text{ and all } u \geq u_0.$$

Suppose further that there are constants  $C', K, b' \geq 0$  and  $u_* \geq 1$  such that

$$C' \pi(u) \geq \left(\frac{q_n}{n}\right)^K e^{-b'u} \quad \text{for all } u \geq u_*.$$

2. Suppose that there is a constant  $c > 0$  such that  $\int_0^1 \pi(u) du \geq c$ .
3. Let  $s_n = \frac{q_n}{n} \log\left(\frac{n}{q_n}\right)$ , and let  $d_n = \sqrt{\log(n/q_n)}$ . Assume that there is a constant  $C$  such that

$$\int_{s_n}^{\infty} \left(u \wedge \frac{d_n^3}{\sqrt{u}}\right) \pi(u) du + d_n \int_1^{d_n^2} \frac{\pi(u)}{\sqrt{u}} du \leq C s_n. \quad (14)$$

Then, under Conditions 1-3,

$$\sup_{\theta_0 \in \ell_0[q_n]} \mathbb{E}_{\theta_0} \Pi \left( \theta : \|\theta - \theta_0\|^2 > M_n q_n \log\left(\frac{n}{q_n}\right) \mid \mathbf{X} \right) \rightarrow 0,$$

i.e. the posterior distribution under prior (2) contracts at the minimax contraction rate.

To briefly summarize, Condition 1 of Proposition 2 assumes that the posterior recovers nonzero means at optimal rate by ensuring that the tails decay no faster than at exponential rate. Condition 2 ensures that  $\pi$  puts some finite mass on values between  $[0, 1]$ . Finally, Condition 3 describes the decay of  $\pi$  away from a neighborhood of zero. One easily checks that the IGG prior satisfies both the first two conditions for any  $a \in (\frac{1}{2}, \infty)$  and appropriately chosen  $b$ , but it does not necessarily satisfy the third one, as we show in the below lemma.

**Lemma 1.** *Suppose that we observe  $\mathbf{X} = (X_1, \dots, X_n) \sim \mathcal{N}(\theta_0, \mathbf{I}_n)$ . Suppose that  $a \in (\frac{1}{2}, \infty)$  and  $b \in (0, 1)$  is a sequence such that  $b = o(1)$ . Then the prior density on the scale term in the IGG prior with hyperparameters  $(a, b)$  fails to satisfy Condition 3 in Proposition 2.*

*Proof.* See Appendix B. □

Lemma 1 shows that if  $a \in (\frac{1}{2}, \infty)$ , then for any  $b \in (0, 1)$  where  $b = o(1)$ , the  $\text{IGG}_n$  prior does not satisfy the conditions given by van der Pas et al. [25]. However, as we show in Theorem 6, for  $a \in (\frac{1}{2}, \infty)$ , the IGG posterior does in fact contract at minimax rate, provided that an appropriate rate of decay is placed on  $b$ . Therefore, we have shown that while the conditions

given in Proposition 2 are sufficient for minimax posterior contraction for the sparse normal means problem, they are not necessary.

We next study the mean square error (MSE) and the posterior variance of the IGG prior and provide an upper bound on both. For all our results, we assume that the true  $\theta_0$  belongs to the set of nearly black vectors defined by (10). With a suitably chosen rate for  $b_n$  in (9), these upper bounds are equal, up to a multiplicative constant, to the minimax risk. Utilizing these bounds, we also show that the posterior distribution under the IGG<sub>n</sub> prior (9) is able to contract around  $\theta_0$  at minimax-optimal rates.

Since the priors (9) are independently placed on each  $\theta_i, i = 1, \dots, n$ , we denote the resulting vector of posterior means  $(\mathbb{E}(\theta_1|X_1), \dots, \mathbb{E}(\theta_n|X_n))$  by  $T(\mathbf{X})$  and the  $i$ th individual posterior mean by  $T(X_i)$ . Therefore,  $T(\mathbf{X})$  is the Bayes estimate of  $\theta$  under squared error loss. Theorem 4 gives an upper bound on the mean squared error for  $T(\mathbf{X})$ .

**Theorem 4.** *Suppose  $\mathbf{X} \sim \mathcal{N}(\theta_0, \mathbf{I}_n)$ , where  $\theta_0 \in \ell_0[q_n]$ . Let  $T(\mathbf{X})$  denote the posterior mean vector under (9). If  $a \in (\frac{1}{2}, \infty)$ ,  $b_n \in (0, 1)$  with  $b_n \rightarrow 0$  as  $n \rightarrow \infty$ , the MSE satisfies*

$$\sup_{\theta_0 \in \ell_0[q_n]} \mathbb{E}_{\theta_0} \|T(\mathbf{X}) - \theta_0\|^2 \lesssim q_n \log\left(\frac{1}{b_n}\right) + (n - q_n)b_n \sqrt{\log\left(\frac{1}{b_n}\right)},$$

provided that  $q_n \rightarrow \infty$  and  $q_n = o(n)$  as  $n \rightarrow \infty$ .

*Proof.* See Appendix B. □

By the minimax result in Donoho et al. [13], we also have the lower bound,

$$\sup_{\theta_0 \in \ell_0[q_n]} \mathbb{E}_{\theta_0} \|T(\mathbf{X}) - \theta_0\|^2 \geq 2q_n \log\left(\frac{n}{q_n}\right) (1 + o(1)),$$

as  $n, q_n \rightarrow \infty$  and  $q_n = o(n)$ . The choice of  $b_n = \left(\frac{q_n}{n}\right)^\alpha$ , for  $\alpha \geq 1$ , therefore leads to an upper bound MSE of order  $q_n \log\left(\frac{n}{q_n}\right)$  with a multiplicative constant of at most  $2\alpha$ . Based on these observations, we immediately have the following corollary.

**Corollary 4.1.** *Suppose that  $q_n$  is known, and that we set  $b_n = \left(\frac{q_n}{n}\right)^\alpha$ , where  $\alpha \geq 1$ . Then under the conditions of Theorem 4,*

$$\sup_{\theta_0 \in \ell_0[q_n]} \mathbb{E}_{\theta_0} \|T(\mathbf{X}) - \theta_0\|^2 \asymp q_n \log\left(\frac{n}{q_n}\right).$$

Corollary 4.1 shows that the posterior mean under the IGG prior performs well as a point estimator for  $\theta_0$ , as it is able to attain the minimax risk (possibly up to a multiplicative constant of at most 2 for  $\alpha = 1$ ). Although the IGG prior does not include a point mass at zero, Proposition 1 and Corollary 4.1 together show that the pole at zero for the IGG prior mimics the point mass well enough, while the heavy tails ensure that large observations are not over-shrunk.

The next theorem gives an upper bound for the total posterior variance corresponding to the IGG<sub>n</sub> (9) prior.

**Theorem 5.** *Suppose  $\mathbf{X} \sim \mathcal{N}(\theta_0, \mathbf{I}_n)$ , where  $\theta_0 \in \ell_0[q_n]$ . Under prior (7) and the conditions of Theorem 4, the total posterior variance satisfies*

$$\sup_{\theta_0 \in \ell_0[q_n]} \mathbb{E}_{\theta_0} \sum_{i=1}^n \text{Var}(\theta_{0i} | X_i) \lesssim q_n \log \left( \frac{1}{b_n} \right) + (n - q_n) b_n \sqrt{\log \left( \frac{1}{b_n} \right)},$$

provided that  $q_n \rightarrow \infty$  and  $q_n = o(n)$  as  $n \rightarrow \infty$ .

*Proof.* See Appendix B. □

Having proven Theorems 4 and 5, we are now ready to state our main theorem concerning optimal posterior contraction. Theorem 6 shows that the IGG is competitive with other popular heavy-tailed priors like the global-local shrinkage priors considered in Ghosh and Chakrabarti [16] or the Dirichlet-Laplace prior considered by Bhattacharya et al. [6]. As before, we denote the posterior mean vector under (9) as  $T(\mathbf{X})$ .

**Theorem 6.** *Suppose  $\mathbf{X} \sim \mathcal{N}(\theta_0, \mathbf{I}_n)$ , where  $\theta_0 \in \ell_0[q_n]$ . Suppose that the true sparsity level  $q_n$  is known, with  $q_n \rightarrow \infty$ , and  $q_n = o(n)$  as  $n \rightarrow \infty$ . Under prior (9), with  $a \in (\frac{1}{2}, \infty)$  and  $b_n = (\frac{q_n}{n})^\alpha, \alpha \geq 1$ ,*

$$\sup_{\theta_0 \in \ell_0[q_n]} \mathbb{E}_{\theta_0} \Pi \left( \theta : \|\theta - \theta_0\|^2 > M_n q_n \log \left( \frac{n}{q_n} \right) \middle| \mathbf{X} \right) \rightarrow 0, \quad (15)$$

and

$$\sup_{\theta_0 \in \ell_0[q_n]} \mathbb{E}_{\theta_0} \Pi \left( \theta : \|\theta - T(\mathbf{X})\|^2 > M_n q_n \log \left( \frac{n}{q_n} \right) \middle| \mathbf{X} \right) \rightarrow 0, \quad (16)$$

for every  $M_n \rightarrow \infty$  as  $n \rightarrow \infty$ .

*Proof.* A straightforward application of Markov's inequality combined with the results of Theorems 4 and 5 leads to (15), while (16) follows from Markov's inequality combined with only the result of Theorem 5. □

Theorem 6 shows that under mild regularity conditions, the posterior distribution under the IGG prior contracts around both the true mean vector *and* the corresponding Bayes estimates at least as fast as the minimax  $l_2$  risk in (11). Since the posterior distribution cannot contract around the truth faster than the rate of  $q_n \log\left(\frac{n}{q_n}\right)$  (by Ghosal et al. [15]), the posterior distribution for the IGG prior under the conditions of Theorem 6 must contract around the true  $\theta_0$  at the minimax optimal rate in (11) up to some multiplicative constant.

We remark that the conditions needed to attain the minimax rate of posterior contraction are quite mild. Namely, we only require that  $q_n = o(n)$ , and we do not need to make any assumptions on the size of the true signal size or the sparsity level. For comparison, Castillo and van der Vaart [10] showed that the spike-and-slab prior with a Gaussian slab contracts at sub-optimal rate if  $\|\theta_0\|^2 \gtrsim q_n \log\left(\frac{n}{q_n}\right)$ . Bhattacharya et al. [6] showed that given the  $\text{Dir}(a, \dots, a)$  prior in the Dirichlet-Laplace prior, the posterior contracts around  $\theta_0$  at the minimax rate, provided that  $\|\theta_0\|_2^2 \leq q_n \log^4 n$  if  $a = n^{-(1+\beta)}$ , or provided that  $q_n \gtrsim \log n$  if  $a = \frac{1}{n}$ . The  $\text{IGG}_n$  prior (9) removes these restrictions on  $\theta_0$  and  $q_n$ . Moreover, our minimax contraction result does not rely on tuning or estimating a global tuning parameter  $\tau$ , as many previous authors have done, but instead, on appropriate selection of hyperparameters  $a$  and  $b$  in the Bayesian hierarchy for the product density of an  $\mathcal{IG}(a, 1)$  and  $\mathcal{G}(b, 1)$ .

In reality, the true sparsity level of  $q_n$  is rarely known, so the best that we can do is to obtain the near-minimax contraction rate of  $q_n \log n$ . A suitable modification of Theorem 6 leads to the following corollary.

**Corollary 6.1.** *Suppose  $\mathbf{X} \sim \mathcal{N}(\theta_0, \mathbf{I}_n)$ , where  $\theta_0 \in \ell_0[q_n]$ . Suppose that the true sparsity level  $q_n$  is unknown, but that  $q_n \rightarrow \infty$ , and  $q_n = o(n)$  as  $n \rightarrow \infty$ . Under prior (9), with  $a \in (\frac{1}{2}, \infty)$  and  $b_n = \frac{1}{n^\alpha}$ ,  $\alpha \geq 1$ , then*

$$\sup_{\theta_0 \in \ell_0[q_n]} \mathbb{E}_{\theta_0} \Pi \left( \theta : \|\theta - \theta_0\|^2 > M_n q_n \log n \mid \mathbf{X} \right) \rightarrow 0, \quad (17)$$

and

$$\sup_{\theta_0 \in \ell_0[q_n]} \mathbb{E}_{\theta_0} \Pi \left( \theta : \|\theta - T(\mathbf{X})\|^2 > M_n q_n \log n \mid \mathbf{X} \right) \rightarrow 0, \quad (18)$$

for every  $M_n \rightarrow \infty$  as  $n \rightarrow \infty$ .

Having shown that the posterior mean under (9) attains the minimax risk up to a multiplicative constant, and that its posterior density captures the

true  $\theta_0$  in a ball of squared radius at most  $q_n \log n$  up to some multiplicative constant, we now quantify its shrinkage profile around zero in terms of Kullback-Leibler risk bounds. We show that this risk bound is in fact sharper than other known shrinkage priors.

### 3.3 Kullback-Leibler Risk Bounds

In Section 3.2, we established that the choice of  $b_n = \frac{1}{n}$  allows the  $\text{IGG}_n$  posterior to contract at near minimax rate, provided that  $a \in (\frac{1}{2}, \infty)$ . Figure 1 suggests that the shrinkage around zero is more aggressive for the  $\text{IGG}_n$  prior than it is for other known shrinkage priors when  $a$  and  $b$  are both set to small values. In this section, we provide a theoretical justification for this behavior near zero.

Carvalho et al. [9] and Bhadra et al. [5] showed that when the true data generating model is  $\mathcal{N}(\mathbf{0}, \mathbf{I}_n)$ , the Bayes estimate for the sampling density of the horseshoe and the horseshoe+ estimators converge to the true model at a super-efficient rate in terms of the Kullback-Leibler (K-L) distance between the true model and the posterior density. They argue that as a result, the horseshoe and horseshoe+ estimators squelch noise better than other shrinkage estimators. However, in this section, we show that the  $\text{IGG}_n$  prior is able to shrink noise even more aggressively with appropriate chosen  $b_n$ .

Let  $\theta_0$  be the true parameter value and  $f(y|\theta)$  be the sampling model. Further, let  $K(q_1, q_2) = \mathbb{E}_{q_1} \log(q_1/q_2)$  denote the K-L divergence of the density  $q_2$  from  $q_1$ . The proof utilizes the following result by Clarke and Barron [11].

**Proposition 3.** (Clarke and Barron, 1990). *Let  $\nu_n(d\theta|y_1, \dots, y_n)$  be the posterior distribution corresponding to some prior  $\nu(d\theta)$  after observing data  $y_{(n)} = (y_1, \dots, y_n)$  according to the sampling model  $f(y|\theta)$ . Define the posterior predictive density  $\hat{q}_n(y) = \int f(y|\theta)\nu_n(d\theta|y_1, \dots, y_n)$ . Assume further that  $\nu(A_\epsilon) > 0$  for all  $\epsilon > 0$ . Then the Cesàro-average risk of the Bayes estimator, define as  $R_n \equiv n^{-1} \sum_{j=1}^n K(q_{\theta_0}, \hat{q}_j)$ , satisfies*

$$R_n \leq \epsilon - \frac{1}{n} \log \nu(A_\epsilon),$$

where  $\nu(A_\epsilon)$  denotes the measure of the set  $\{\theta : K(q_{\theta_0}, q_\theta) \leq \epsilon\}$ .

Using the above proposition, it is shown in Carvalho et al. [9] and Bhadra et al. [5] that when the global parameter  $\tau$  is fixed at  $\tau = 1$  and the true



parameter  $\theta_0 = 0$ , the horseshoe and the horseshoe+ both have Cesàro-average risk which satisfies

$$R_n = O\left(\frac{1}{n} \log\left(\frac{n}{(\log n)^d}\right)\right), \quad (19)$$

where  $d$  is a positive constant. This rate is super-efficient, in the sense that the risk is lower than that of the maximum likelihood estimator (MLE), which has the rate  $O(\log n/n)$  when  $\theta_0 = \mathbf{0}$ . The next theorem establishes that the IGG prior can achieve an even faster rate of convergence  $O(n^{-1})$  in the K-L sense, with appropriate choices of  $a$  and  $b$ .

**Theorem 7.** *Suppose that the true sampling model  $p_{\theta_0}$  is  $y_j \sim N(\theta_0, 1)$ . Then for  $\hat{q}_n$  under the IGG prior with any  $a > 0$  and  $b_n = \frac{1}{n}$ , the optimal rate of convergence of  $R_n$  when  $\theta_0 = 0$  satisfies the inequality,*

$$R_n \leq \frac{1}{n} \left[ 2 + \log(\sqrt{\pi}) + (a + 2) \log(2) + \log\left(a + \frac{1}{2}\right) \right] + \frac{2 \log n}{n^2}, \quad (20)$$

*Proof.* See Appendix C. □

Since  $\frac{\log n}{n^2} = o(n^{-1})$ , we see from Theorem 7 that the  $\text{IGG}_n$  posterior density with hyperparameters  $a > 0$  and  $b_n = \frac{1}{n}$  has an optimal convergence rate of  $O(n^{-1})$ . This convergence rate is faster than that of the horseshoe or horseshoe+, both of which converge at the rate of  $O\{n^{-1}(\log n - d \log \log n)\}$  when  $\theta_0 = 0$ . To our knowledge, this is the sharpest known bound on Cesàro-average risk for any Bayes estimator. Our result provides a rigorous explanation for the observation that the IGG seems to shrink noise more aggressively than other scale-mixture shrinkage priors.

Theorem 7 not only justifies the use of  $b_n = \frac{1}{n}$  as a choice for hyperparameter  $b$  in the IGG prior, but it also provides insight into how we should choose the hyperparameter  $a$ . (20) shows that the constant  $C$  in  $R_n \leq Cn^{-1} + o(n^{-1})$  can be large if  $a$  is set to be large. This theorem thus implies that in order to minimize the K-L distance between  $\mathcal{N}(\theta_0, \mathbf{I}_n)$  and the IGG posterior density, we should pick  $a$  to be small. Since we require  $a \in (\frac{1}{2}, \infty)$  in order to achieve the near-minimax contraction rate, our theoretical results suggest that we should set  $a \in (\frac{1}{2}, \frac{1}{2} + \delta]$  for small  $\delta > 0$  for optimal posterior concentration.

## 4 Multiple Testing with the IGG Prior

### 4.1 Asymptotic Bayes Optimality Under Sparsity

Suppose we observe  $\mathbf{X} = (X_1, \dots, X_n)$ , such that  $X_i \sim N(\theta_i, 1)$ , for  $i = 1, \dots, n$ . To identify the true signals in  $\mathbf{X}$ , we conduct  $n$  simultaneous tests:  $H_{0i} : \theta_i = 0$  against  $H_{1i} : \theta_i \neq 0$ , for  $i = 1, \dots, n$ . For each  $i$ ,  $\theta_i$  is assumed to be generated by a true data-generating model,

$$\theta_i \stackrel{i.i.d.}{\sim} (1-p)\delta_{\{0\}} + pN(0, \psi^2), i = 1, \dots, n, \quad (21)$$

where  $\psi^2 > 0$  represents a diffuse “slab” density. This point mass mixture model is often considered a theoretical ideal for generating a sparse vector  $\boldsymbol{\theta}$  in the statistical literature. Indeed, Carvalho et al. [8] referred to model (21) as a “gold standard” for sparse problems.

Model (21) is equivalent to assuming that for each  $i$ ,  $\theta_i$  follows a random variable whose distribution is determined by the latent binary random variable  $\nu_i$ , where  $\nu_i = 0$  denotes the event that  $H_{0i}$  is true, while  $\nu_i = 1$  corresponds to the event that  $H_{0i}$  is false. Here  $\nu_i$ ’s are assumed to be i.i.d. Bernoulli( $p$ ) random variables, for some  $p$  in  $(0, 1)$ . Under  $H_{0i}$ , i.e.  $\theta_i \sim \delta_{\{0\}}$ , the distribution having a mass 1 at 0, while under  $H_{1i}$ ,  $\theta_i \neq 0$  and is assumed to follow an  $N(0, \psi^2)$  distribution with  $\psi^2 > 0$ . The marginal distributions of the  $X_i$ ’s are then given by the following two-groups model:

$$X_i \stackrel{i.i.d.}{\sim} (1-p)N(0, 1) + pN(0, 1 + \psi^2), i = 1, \dots, n. \quad (22)$$

Our testing problem is now equivalent to testing simultaneously

$$H_{0i} : \nu_i = 0 \text{ versus } H_{1i} : \nu_i = 1 \text{ for } i = 1, \dots, n. \quad (23)$$

We consider a symmetric 0-1 loss for each individual test and the total loss of a multiple testing procedure is assumed to be the sum of the individual losses incurred in each test. Letting  $t_{1i}$  and  $t_{2i}$  denote the probabilities of type I and type II errors of the  $i$ th test respectively, the Bayes risk of a multiple testing procedure under the two-groups model (1) is given by

$$R = \sum_{i=1}^m \{(1-p)t_{1i} + pt_{2i}\}. \quad (24)$$

Bogdan et al. [7] showed that the rule which minimizes the Bayes risk in (24) is the test which, for each  $i = 1, \dots, n$ , rejects  $H_{0i}$  if

$$\frac{f(x_i|\nu_i = 1)}{f(x_i|\nu_i = 0)} > \frac{1-p}{p}, \text{ i.e. } X_i^2 > c^2, \quad (25)$$

where  $f(x_i|\nu_i = 1)$  denotes the marginal density of  $X_i$  under  $H_{1i}$ , while  $f(x_i|\nu_i = 0)$  denotes that under  $H_{0i}$  and  $c^2 \equiv c_{\psi, f}^2 = \frac{1+\psi^2}{\psi^2}(\log(1 + \psi^2) + 2\log(f))$ , with  $f = \frac{1-p}{p}$ . The above rule is known as the Bayes Oracle, because it makes use of unknown parameters  $\psi$  and  $p$ , and hence, it is not attainable in finite samples. By reparametrizing as  $u = \psi^2$  and  $v = uf^2$ , the above threshold becomes

$$c^2 \equiv c_{u,v}^2 = \left(1 + \frac{1}{u}\right) \left(\log v + \log \left(1 + \frac{1}{u}\right)\right).$$

Bogdan et al. [7] considered the following asymptotic scheme.

### Assumption 1

The sequences of vectors  $(\psi_n, p_n)$  satisfies the following conditions:

1.  $p_n \rightarrow 0$  as  $n \rightarrow \infty$ .
2.  $u_n = \psi_n^2 \rightarrow \infty$  as  $n \rightarrow \infty$ .
3.  $v_n = u_n f^2 = \psi_n^2 \left(\frac{1-p_n}{p_n}\right)^2 \rightarrow \infty$  as  $n \rightarrow \infty$ .
4.  $\frac{\log v_n}{u_n} \rightarrow C \in (0, \infty)$  as  $n \rightarrow \infty$ .

Bogdan et al. [7] provided detailed insight on the threshold  $C$ . Summarizing briefly, if  $C = 0$ , then both the Type I and Type II errors are zero, and for  $C = \infty$ , the inference is essentially no better than tossing a coin. Under Assumption 1, Bogdan et al. [7] showed that the corresponding asymptotic optimal Bayes risk has a particularly simple form, which is given by

$$R_{Opt}^{BO} = n((1-p)t_1^{BO} + pt_2^{BO}) = np(2\Phi(\sqrt{C}) - 1)(1 + o(1)), \quad (26)$$

where the  $o(1)$  terms tend to zero as  $n \rightarrow \infty$ . A testing procedure with risk  $R$  is said to be asymptotically Bayes optimal under sparsity (ABOS) if

$$\frac{R}{R_{Opt}^{BO}} \rightarrow 1 \text{ as } n \rightarrow \infty. \quad (27)$$

## 4.2 An Optimal Testing Rule Based on the IGG Estimator

As noted earlier, the posterior mean depends heavily on the shrinkage factor,  $\kappa_i = \frac{1}{\lambda_i \xi_i + 1}$ . Because of the concentration properties of the IGG prior proven in Sections 2.1 and 3, a sensible thresholding rule classifies observations as

signals or as noise based on the posterior distribution of this shrinkage factor. Consider the following testing rule for the  $i$ th observation  $X_i$ :

$$\text{Reject } H_{0i} \text{ if } \mathbb{E}(1 - \kappa_i | X_i) > \frac{1}{2}, \quad (28)$$

where  $\kappa_i$  is the shrinkage factor based on the  $IGG_n$  prior (9). Within the context of multiple testing, a good benchmark for our test procedure (28) should be whether it is ABOS, i.e. whether its optimal risk is asymptotically equal to that of the Bayes Oracle risk. Adopting the framework of Bogdan et al. [7], we let  $R_{IGG}$  denote the asymptotic Bayes risk of testing rule (28), and we compare it to the ABOS risk defined in (26).

The next theorem illustrates that in the presence of sparsity, rule (28) is in fact ABOS.

**Theorem 8.** *Suppose that  $X_1, \dots, X_n$  are i.i.d. observations having distribution (22) where the sequence of vectors  $(\psi^2, p)$  satisfies Assumption 1. Suppose we wish to test (23) using the classification rule (28). Suppose further that  $a \in (\frac{1}{2}, \infty)$  and  $b_n \in (0, 1)$ , with  $b_n \rightarrow 0$  as  $n \rightarrow \infty$  in such a way that  $\lim_{n \rightarrow \infty} \frac{b_n^{1/4}}{p_n} \in (0, \infty)$ . Then*

$$\lim_{n \rightarrow \infty} \frac{R_{IGG}}{R_{Opt}^{BO}} = 1, \quad (29)$$

i.e. rule (28) based on the  $IGG_n$  prior (9) is ABOS.

*Proof.* See Appendix D. □

We have shown that our thresholding rule based on the  $IGG_n$  prior asymptotically attains the ABOS risk exactly, provided that  $b_n$  decays to zero at a certain rate relative to the sparsity level  $p$ . For example, if the prior mixing proportion  $p_n$  is known, we can set the hyperparameter  $b_n = p_n^4$ . Then the conditions for classification rule (28) to be ABOS are satisfied.

Our work ultimately moves the testing problem beyond the global-local framework. Previously, Datta and Ghosh [12], Ghosh et al. [17], Bhadra et al. [5], and Ghosh and Chakrabarti [16]) have shown that horseshoe or horseshoe-like priors asymptotically attain the Bayes Oracle risk (possibly up to a multiplicative constant) either by specifying a rate for the global parameter  $\tau$  in (3) or by estimating it with an empirical Bayes plug-in estimator. In the case with the  $IGG$  prior, we prove that our thresholding rule based on the posterior mean is ABOS without utilizing a shared global tuning parameter.

## 5 Simulation Studies

### 5.1 Computation and Selection of Hyperparameters

Letting  $\kappa_i = \frac{1}{1+\lambda_i\xi_i}$ , the full conditional distributions for (8) are

$$\begin{aligned}\theta_i \mid \text{rest} &\sim N((1 - \kappa_i)X_i, 1 - \kappa_i), i = 1, \dots, n, \\ \lambda_i \mid \text{rest} &\sim \mathcal{IG}\left(a + \frac{1}{2}, \frac{\theta_i^2}{2\xi_i} + 1\right), i = 1, \dots, n, \\ \xi_i \mid \text{rest} &\sim \text{giG}\left(\frac{\theta_i^2}{\lambda_i}, 2, b - \frac{1}{2}\right), i = 1, \dots, n,\end{aligned}\tag{30}$$

where  $\text{giG}(a, b, p)$  denotes a generalized inverse Gaussian (giG) density with  $f(x; a, b, p) \propto x^{(p-1)}e^{-(a/x+bx)/2}$ . Therefore, the IGG model (8) can be implemented straightforwardly with Gibbs sampling, utilizing the full conditionals in (30).

For all our simulations, we set  $a = \frac{1}{2} + \frac{1}{n}$  and  $b = \frac{1}{n}$ , in light of Theorems 6 and 7. These choices of  $a$  and  $b$  ensure that the IGG posterior will contract around the true  $\theta_0$  at least at near-minimax rate, while keeping  $a \in (\frac{1}{2}, \infty)$  small. We denote our IGG prior with hyperparameters  $(a, b) = (\frac{1}{2} + \frac{1}{n}, \frac{1}{n})$  as  $\text{IGG}_{1/n}$ . For both of the simulation studies described below, we run 10,000 iterations of a Gibbs sampler, discarding the first 5000 as burn-in.

### 5.2 Simulation Study for Sparse Estimation

To illustrate finite-sample performance of the  $\text{IGG}_{1/n}$  prior, we use the set-up in Bhadra et al. [5] where we specify sparsity levels of  $q/n = 0.05, 0.10, 0.20$ , and  $0.30$ , and set the signals all equal to values of either  $A = 7$  or  $8$ , for a total of eight simulation settings. With  $n = 200$ , we randomly generate  $n$ -dimensional vectors under these settings and compute the average squared error loss corresponding to the posterior median across 100 replicates.

We compare our results for  $\text{IGG}_{1/n}$  to the average squared error loss of the posterior median under the Dirichlet-Laplace (DL), the horseshoe (HS), and the horseshoe+ (HS+) estimators, since these are global-local shrinkage priors (3) with singularities at zero. For the HS and HS+ priors, we use a fully Bayesian approach, with  $\tau \sim C^+(0, 1)$ , as in Ghosh et al. [17]. For the DL prior, we specify  $a = \frac{1}{n}$  in the  $\text{Dir}(a, \dots, a)$  prior of the scale component, along with  $\tau \sim \mathcal{G}(na, 1/2)$ , as in Bhattacharya et al. [6]. Our results are presented in Table 1.

Table 1 shows that under these various sparsity and signal strength settings, the  $\text{IGG}_{1/n}$ 's posterior median has the lowest (estimated) squared error loss in nearly all of the simulation settings. It performs better than the

q/n	A	IGG	DL	HS	HS+
0.05	7	<b>13.88</b>	14.30	18.11	14.41
	8	13.34	<b>13.27</b>	17.71	13.96
0.10	7	<b>27.21</b>	29.91	35.91	30.18
	8	<b>25.95</b>	27.67	34.77	29.36
0.20	7	<b>49.78</b>	56.40	71.18	58.25
	8	<b>47.24</b>	52.22	69.81	57.11
0.30	7	<b>74.42</b>	85.72	104.67	86.00
	8	<b>70.83</b>	79.03	104.02	84.70

Table 1: Comparison of average squared error loss for the posterior median estimate of  $\theta$  across 100 replications. Results are reported for the  $\text{IGG}_{1/n}$ , DL (Dirichlet-Laplace), HS (horseshoe), and the HS+ (horseshoe-plus).

horseshoe and the horseshoe+ in all settings. Our empirical results confirm the theoretical properties that were proven in Section 3 and illustrate that for finite samples, the IGG prior often outperforms other popular shrinkage priors. Our empirical results also lend strong support to the use of the inverted beta prior  $\beta'(a, b)$  as the scale density in scale-mixture shrinkage priors (2). However, our results suggest that we can obtain better estimation if we allow the  $a$  and  $b$  to vary with sample size, rather than keeping them fixed (as the horseshoe priors do, with  $a = b = 0.5$ ).

### 5.3 Simulation Study for Multiple Testing

For the multiple testing rule (28), we adopt the simulation framework of Datta and Ghosh [12] and Ghosh et al. [17] and fix sparsity levels at  $p \in \{0.01, 0.05, 0.10, 0.15, 0.2, 0.25, 0.3, 0.35, 0.4, 0.45, 0.5\}$  for a total of 11 simulation settings. For sample size  $n = 200$  and each  $p$ , we generate data from the two-groups model (21), with  $\psi = \sqrt{2 \log n} = 3.26$ . We then apply the thresholding rule (28) using  $\text{IGG}_{1/n}$  to classify  $\theta_i$ 's in our model as either signals ( $\theta_i \neq 0$ ) or noise ( $\theta_i = 0$ ). We estimate the average misclassification probability (MP) for the thresholding rule (28) from 100 replicates.

Taking  $p = 0.10$ , we plot in Figure 2 the theoretical posterior inclusion probabilities  $\omega_i(X_i) = P(\nu_i = 1|X_i)$  for the two-groups model (21) given by

$$\omega_i(X_i) = \pi(\nu_i = 1|X_i) = \left\{ \left( \frac{1-p}{p} \right) \sqrt{1 + \psi^2} e^{-\frac{X_i^2}{2} \frac{\psi^2}{1+\psi^2}} + 1 \right\}^{-1},$$

along with the shrinkage weights  $1 - \mathbb{E}(\kappa_i|X_i)$  corresponding to the  $\text{IGG}_{1/n}$

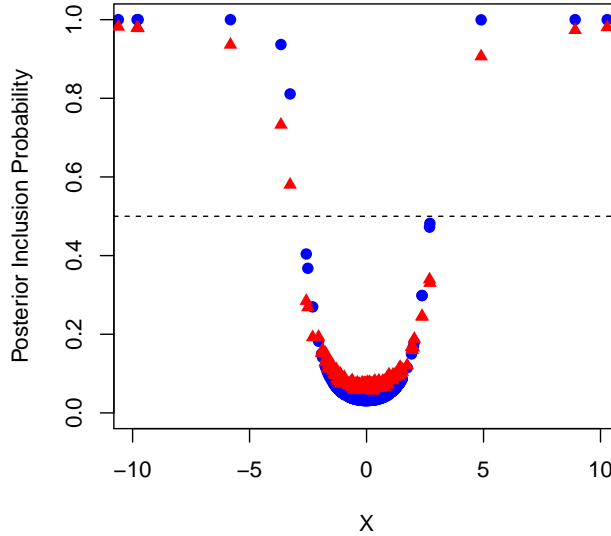


Figure 2: Comparison between the posterior inclusion probabilities and the posterior shrinkage weights  $1 - \mathbb{E}(\kappa_i|X_i)$  when  $p = 0.10$ .

prior. The circles in the figure denote the theoretical posterior inclusion probabilities, while the triangles correspond to the shrinkage weights  $1 - \mathbb{E}(\kappa_i|X_i)$ . The figure clearly shows that for small values of the sparsity level  $p$ , the shrinkage weights are in close proximity to the posterior inclusion probabilities. This and the theoretical results established in Section 4 justify the use of using  $1 - \mathbb{E}(\kappa_i|X_i)$  as an approximation to the corresponding posterior inclusion probabilities  $\omega_i(X_i)$  in sparse situations. Therefore, this motivates the use of the  $\text{IGG}_{1/n}$  prior (9) and its corresponding decision rule (28) for identifying signals in noisy data.

Figure 3 shows the estimated misclassification probabilities (MP) for decision rule (28) for the  $\text{IGG}_{1/n}$  prior, along with the estimated MP's for the Bayes Oracle (BO), the Benjamini-Hochberg procedure (BH), the Dirichlet-Laplace (DL), the horseshoe (HS), and the horseshoe+ (HS+). The Bayes Oracle rule, defined in (25), is the decision rule that minimizes the expected number of misclassified signals (24) when  $(p, \psi)$  are known. The Bayes Oracle therefore serves as the lower bound to the MP, whereas the line  $MP = p$  corresponds to the situation where we reject all null hypotheses without looking into the data. For the Benjamini-Hochberg rule, we use  $\alpha_n = 1/\log n = 0.1887$ . Bogdan et al. [7] theoretically established the ABOS property of the BH procedure for this choice of  $\alpha_n$ . For the DL, HS,

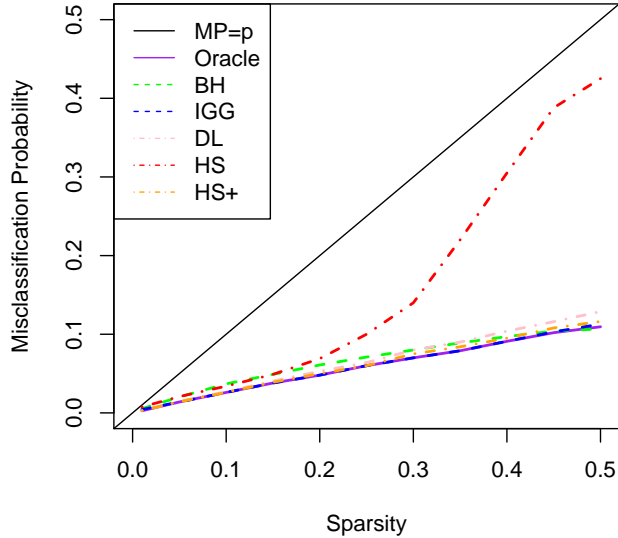


Figure 3: Estimated misclassification probabilities. Thresholding rule (28) based on the IGG posterior mean is nearly as good as the Bayes Oracle (25).

and HS+ priors, we use the classification rule

$$\text{Reject } H_{0i} \text{ if } \mathbb{E}(1 - \kappa_i | X_1, \dots, X_n) > \frac{1}{2}, \quad (31)$$

where  $\kappa_i = \frac{1}{1 + \sigma_i^2}$  and  $\sigma_i^2$  is the scale parameter in the scale-mixture shrinkage model (2). For the horseshoe and horseshoe+ priors, we specify a half-Cauchy prior on the global parameter  $\tau \sim C^+(0, 1)$ . Since  $\tau$  is a shared global parameter, the posterior for  $\kappa_i$  depends on *all* the data. Carvalho et al. [9] first introduced thresholding rule (31) for the horseshoe. Ghosh et al. [17] later extended rule (31) for a general class of global-local shrinkage priors (3), which includes the Strawderman-Berger, normal-exponential-gamma, and generalized double Pareto priors. Based on Ghosh et al. [17]’s simulation results, the horseshoe performs similarly as or better than these other aforementioned priors, so we do not include these other priors in our comparison study.

Our results provide strong support to our theoretical findings in Section 4 and strong justification for the use of (28) to classify signals. As Figure 3 illustrates, the misclassification probability for the IGG prior with  $(a, b) = (\frac{1}{2} + \frac{1}{n}, \frac{1}{n})$  is practically indistinguishable from the Bayes Oracle, which gives the lowest possible MP. Thresholding rule (31) based on the horseshoe+



p	BO	BH	IGG	DL	HS	HS+
0.30	0.08	0.13	0.005	0.08	0.14	0.09
0.35	0.08	0.12	0.004	0.09	0.22	0.10
0.40	0.09	0.11	0.004	0.10	0.31	0.10
0.45	0.10	0.10	0.003	0.12	0.39	0.11
0.50	0.10	0.09	0.003	0.13	0.43	0.11

Table 2: Comparison of false discovery rate (FDR) for different classification methods under dense settings. The  $\text{IGG}_{1/n}$  has the lowest FDR of all the different methods.

prior and the Dirichlet-Laplace priors also appears to be quite competitive compared to the Bayes Oracle. Bhadra et al. [5] proved that the horseshoe+ prior asymptotically matches the Bayes Oracle risk up to a multiplicative constant if  $\tau$  is treated as a tuning parameter, but did not prove this for the case where  $\tau$  is endowed with a prior. There also does not appear to be any theoretical justification for thresholding rule (31) under the DL prior in the literature. On the other hand, Theorem 8 provides theoretical support for the use of (28) under the IGG prior, which is confirmed by our empirical study.

Figure 3 also shows that the performance for rule (31) under the horseshoe degrades considerably as  $\boldsymbol{\theta} = (\theta_1, \dots, \theta_n)$  becomes more dense. With sparsity level  $p = 0.5$ , the horseshoe’s misclassification rate is close to 0.4, only marginally better than rejecting all the null hypotheses without looking at the data. This phenomenon was also observed by Datta and Ghosh [12] and Ghosh et al. [17]. This appears to be because in the dense setting, there are many noisy entries that are “moderately” far from zero, and the horseshoe prior does not shrink these aggressively enough towards zero in order for testing rule (31) to classify these as true noise. The horseshoe+ prior seems to alleviate this by adding an additional half-Cauchy  $C^+(0, 1)$  prior to the Bayes hierarchy. In Table 2, we report the false discovery rate (FDR) under dense settings for the different methods. We see that the FDR is quite a bit larger for the horseshoe than for the other methods. Table 2 also shows that the  $\text{IGG}_{1/n}$  prior has very tight control over the FDR in dense settings. Although the IGG prior is not constructed to specifically control FDR, we see that in practice, it does provide excellent control of false positives.

Finally, we demonstrate the shrinkage properties corresponding to the  $\text{IGG}_{1/n}$  prior along with the horseshoe, the horseshoe+, and the Dirichlet-

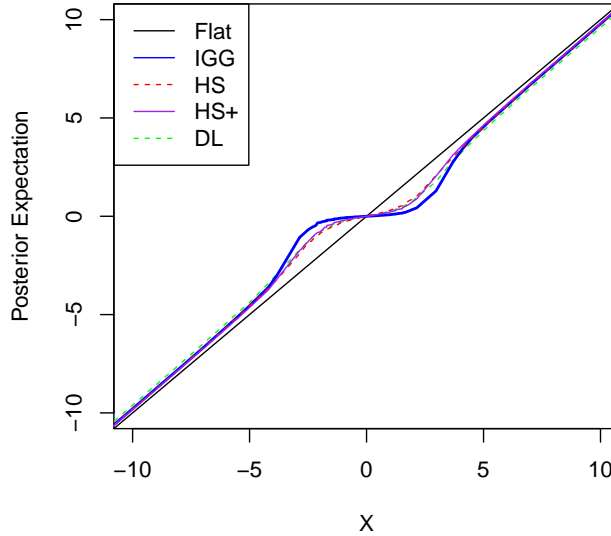


Figure 4: Posterior Mean  $\mathbb{E}(\theta|X)$  vs.  $X$  plot for  $p = 0.25$ .

Laplace priors. In Figure 4, we plot the posterior expectations  $\mathbb{E}(\theta_i|X_i)$  for the  $IGG_{1/n}$  prior and the posterior expectations  $E(\theta_i|X_1, \dots, X_n)$  for the HS, HS+, and DL priors and the posterior expectations. The amount of posterior shrinkage can be observed in terms of distance between the 45° line and the posterior expectation. Figure 4 clearly shows that near zero, the noisy entries are more aggressively shrunk towards zero for the  $IGG_{1/n}$  prior than for the other priors with poles at zero. This confirms our findings in Theorem 7 which proved that the shrinkage profile near zero is more aggressive for the  $IGG_{1/n}$  prior in the Kullback-Leibler sense than for the HS or HS+ priors. Meanwhile, Figure 4 also shows that the signals are left mostly unshrunk, confirming that the IGG shares the same tail robustness as the other priors. The more aggressive shrinkage of noise explains why the IGG performs better estimation, as we demonstrated in Section 5.2.

## 6 Analysis of a Prostate Cancer Data Set

We demonstrate practical application of the IGG prior using a popular prostate cancer data set introduced by Singh et al. [23]. In this data set, there are gene expression values for  $n = 6033$  genes for  $m = 102$  subjects, with  $m_1 = 50$  normal control subjects and  $m_2 = 52$  prostate cancer patients. We aim to identify genes that are significantly different between control

and cancer patients. This problem can be reformulated as normal means problem (1) by first conducting a two-sample t-test for each gene and then transforming the test statistics  $(t_1, \dots, t_n)$  to z-scores using the inverse normal cumulative distribution function (CDF) transform  $\Phi^{-1}(F_{t_{100}}(t_i))$ , where  $F_{t_{100}}$  denotes the CDF for the Student's t distribution with 100 degrees of freedom. With z-scores  $(z_1, \dots, z_n)$ , our model is now

$$z_i = \theta_i + \epsilon_i, \quad i = 1, \dots, n, \quad (32)$$

where  $\epsilon_i \sim N(0, 1)$ . This allows us to implement the IGG prior on the z-scores to conduct simultaneous testing  $H_{0i} : \theta_i = 0$  vs.  $H_{1i} : \theta_i \neq 0$ ,  $i = 1, \dots, n$ , to identify genes that are significantly associated with prostate cancer. Additionally, we can also estimate  $\boldsymbol{\theta} = (\theta_1, \dots, \theta_n)$ . As argued by Efron [14],  $|\theta_i|$  can be interpreted as the effect size of the  $i$ th gene for prostate cancer. Efron [14] first analyzed model (32) for this particular data set by obtaining empirical Bayes estimates  $\hat{\theta}_i^{Efron}$ ,  $i = 1, \dots, n$ , based on the two-groups model (21). In our analysis, we use the posterior means  $\hat{\theta}_i$ ,  $i = 1, \dots, n$ , to estimate the strength of association.

With our z-scores, we implement the  $IGG_{1/n}$  model with  $(a, b) = (\frac{1}{2} + \frac{1}{n}, \frac{1}{n})$  on model (32) and use classification rule (28) to identify significant genes. For comparison, we also fit this model for the DL, HS, and HS+ priors, and benchmark it to the Benjamini-Hochberg (BH) procedure with FDR  $\alpha$  set to 0.10. The  $IGG_{1/n}$  selects 85 genes as significant, in comparison to 60 genes under the BH procedure. The HS prior selects 62 genes as significant. The HS+ and DL priors select 41 and 42 genes respectively, indicating more conservative estimates. All 60 of the genes flagged as significant by the BH procedure are included in the 85 genes that the IGG prior classifies as significant. On the other hand, the HS prior's conclusions diverge from the BH procedure. Seven genes (genes 11, 377, 637, 805, 1588, 3269, and 4040) are deemed significant by the HS, but not by BH.

Table 3 shows the top 10 genes selected by Efron [14] and their estimated effect size on prostate cancer. We compare Efron [14]'s empirical Bayes posterior mean estimates with the posterior mean estimates under the IGG, DL, HS, and HS+ priors. Our results confirm the tail robustness of the IGG prior. All of the scale-mixture shrinkage priors shrink the estimated effect size for significant genes less aggressively than Efron's procedure. Table 3 also shows that for large signals, the IGG posterior has slightly less shrinkage for large signals than the DL posterior and roughly the same amount as the HS posterior. The HS+ posterior shrinks the test statistics the least for large signals, but the IGG's estimates are still quite similar to those of the HS+.

Gene	z-score	$\hat{\theta}_i^{IGG}$	$\hat{\theta}_i^{DL}$	$\hat{\theta}_i^{HS}$	$\hat{\theta}_i^{HS+}$	$\hat{\theta}_i^{Efron}$
610	5.29	4.85	4.52	4.85	4.91	4.11
1720	4.83	4.33	3.94	4.33	4.35	3.65
332	4.47	3.78	3.40	3.78	3.99	3.24
364	-4.42	-3.78	-3.10	-3.78	-3.85	-3.57
914	4.40	3.71	3.11	3.71	3.86	3.16
3940	-4.33	-3.70	-3.06	-3.70	-3.80	-3.52
4546	-4.29	-3.59	-3.09	-3.59	-3.62	-3.47
1068	4.25	3.49	3.09	3.49	3.46	2.99
579	4.19	3.31	2.98	3.31	3.01	2.92
4331	-4.14	-3.41	-2.87	-3.41	-3.43	-3.30

Table 3: The z-scores and the effect size estimates for the top 10 genes selected by Efron [14] by the IGG, DL, HS, and HS+ models and the two-groups empirical Bayes model by Efron [14].

## 7 Concluding Remarks

In this paper, we have introduced a new scale-mixture shrinkage prior called the Inverse Gamma-Gamma prior for estimating sparse normal mean vectors. This prior has been shown to have a number of good theoretical properties, including heavy probability mass around zero and heavy tails. This enables the IGG prior to perform selective shrinkage and to attain (near) minimax contraction around the true  $\theta$  in (1). The IGG posterior also converges to the true model at a faster rate than the horseshoe and horseshoe+ posterior densities in the Kullback-Leibler sense. The IGG, HS, and HS+ all fall under the class of priors which utilize a beta prime density (4) as a prior on the scale component for model (2). However, our results suggest that there is added flexibility in allowing the parameters  $(a, b)$  in the density (4) to vary with sample size rather than keeping them fixed. This added flexibility leads to excellent empirical performance and obviates the need to estimate a global tuning parameter  $\tau$ .

Moreover, by thresholding the posterior mean, the IGG can be used to identify signals in  $\theta$ . We have investigated the asymptotic risk properties of this classification rule within the decision theoretic framework of Bogdan et al. [7] and established asymptotically optimal theoretical properties for multiple testing. Since we do not specify or estimate a global parameter  $\tau$ , our paper appears to be the first article to establish the ABOS property for a scale-mixture shrinkage prior which does not fall under the global-local

(3) framework.

Our simulation studies demonstrate the IGG’s strong finite sample performance for obtaining sparse estimates of  $\boldsymbol{\theta}$  and for correctly classifying entries in  $\boldsymbol{\theta}$  as either signals or noise. By setting the hyperparameters  $(a, b) = (\frac{1}{2} + \frac{1}{n}, \frac{1}{n})$ , the IGG prior outperforms other popular shrinkage estimators. Finally, we demonstrated practical application of the IGG prior with a prostate cancer data set.

In recent years, Bayesian scale-mixture shrinkage priors have gained a great amount of attention because of their computational efficiency and their ability to mimic point-mass mixtures in obtaining sparse estimates. Our paper contributes to this large body of methodological and theoretical work. There are a few possible future directions for research. For example, the IGG prior can be adapted to other statistical problems such as sparse covariance estimation, variable selection with covariates, and many others. We conjecture that the IGG would satisfy many optimality properties (e.g. model selection consistency, optimal posterior contraction, etc.) if it were utilized in these other contexts.

Despite the absence of a data-dependent global parameter  $\tau$ , the IGG model adapts well to sparsity, performing well under both sparse and dense settings. This seems to be in stark contrast to remarks made by authors like Carvalho et al. [8] who have argued that scale-mixture shrinkage priors which do not contain shared global parameters do not enjoy the benefits of adaptivity. Nevertheless, we could investigate if theoretical and empirical performance can be improved even further by incorporating a global parameter into the IGG framework. We leave these as interesting problems for future research.

## 8 Acknowledgments

The authors would like to thank Dr. Anirban Bhattacharya and Dr. Xueying Tang for sharing their codes, which were modified to generate Figures 1-4.

## A Proofs for Section 2

*Proof of Proposition 1.* The joint distribution of the prior is proportional to

$$\pi(\boldsymbol{\theta}, \boldsymbol{\xi}, \boldsymbol{\lambda}) \propto (\boldsymbol{\lambda}\boldsymbol{\xi})^{-1/2} \exp\left(-\frac{\boldsymbol{\theta}^2}{2\boldsymbol{\lambda}\boldsymbol{\xi}}\right) \boldsymbol{\lambda}^{-a-1} \exp\left(-\frac{1}{\boldsymbol{\lambda}}\right) \boldsymbol{\xi}^{b-1} \exp(-\boldsymbol{\xi})$$

$$\propto \xi^{b-3/2} \exp(-\xi) \lambda^{-a-3/2} \exp\left(-\left(\frac{\theta^2}{2\xi} + 1\right) \frac{1}{\lambda}\right).$$

Thus,

$$\begin{aligned} \pi(\theta, \xi) &\propto \xi^{b-3/2} \exp(-\xi) \int_{\lambda=0}^{\infty} \lambda^{-a-3/2} \exp\left(-\left(\frac{\theta^2}{2\xi} + 1\right) \frac{1}{\lambda}\right) d\lambda \\ &\propto \left(\frac{\theta^2}{2\xi} + 1\right)^{-(a+1/2)} \xi^{b-3/2} e^{-\xi}, \end{aligned}$$

and thus, the marginal density of  $\theta$  is proportional to

$$\pi(\theta) \propto \int_0^{\infty} \left(\frac{\theta^2}{2\xi} + 1\right)^{-(a+1/2)} \xi^{b-3/2} e^{-\xi} d\xi. \quad (33)$$

As  $|\theta| \rightarrow 0$ , the expression in (33) is bounded below by

$$C \int_0^{\infty} \xi^{b-3/2} e^{-\xi} d\xi, \quad (34)$$

where  $C$  is a constant that depends on  $a$  and  $b$ . The integral expression in (34) clearly diverges to  $\infty$  for any  $0 < b \leq 1/2$ . Therefore, (33) diverges to infinity as  $|\theta| \rightarrow 0$ , by the monotone convergence theorem.  $\square$

*Proof of Theorem 1.* From (7), the posterior distribution of  $\kappa_i$  under  $\text{IGG}_n$  is proportional to

$$\pi(\kappa_i | X_i) \exp\left(-\frac{\kappa_i X_i^2}{2}\right) \kappa_i^{a-1/2} (1 - \kappa_i)^{b_n-1}, \quad \kappa_i \in (0, 1). \quad (35)$$

Since  $\exp\left(-\frac{\kappa_i X_i^2}{2}\right)$  is strictly decreasing in  $\kappa_i$  on  $(0, 1)$ , we have

$$\begin{aligned} \mathbb{E}(1 - \kappa_i | X_i) &= \frac{\int_0^1 \kappa_i^{a-1/2} (1 - \kappa_i)^{b_n} \exp\left(-\frac{\kappa_i X_i^2}{2}\right) d\kappa_i}{\int_0^1 \kappa_i^{a-1/2} (1 - \kappa_i)^{b_n-1} \exp\left(-\frac{\kappa_i X_i^2}{2}\right) d\kappa_i} \\ &\leq \frac{e^{X_i^2/2} \int_0^1 \kappa_i^{a-1/2} (1 - \kappa_i)^{b_n} d\kappa_i}{\int_0^1 \kappa_i^{a-1/2} (1 - \kappa_i)^{b_n-1} d\kappa_i} \end{aligned}$$

$$\begin{aligned}
&= e^{X_i^2/2} \frac{\Gamma(a+1/2)\Gamma(b_n+1)}{\Gamma(a+b_n+3/2)} \times \frac{\Gamma(a+b_n+1/2)}{\Gamma(a+1/2)\Gamma(b_n)} \\
&= e^{X_i^2/2} \left( \frac{b_n}{a+b_n+1/2} \right).
\end{aligned}$$

□

*Proof of Theorem 2.* Note that since  $a \in (\frac{1}{2}, \infty)$ ,  $\kappa_i^{a-1/2}$  is increasing in  $\kappa_i$  on  $(0, 1)$ . Additionally, since  $b_n \in (0, 1)$ ,  $(1 - \kappa_i)^{b_n-1}$  is increasing in  $\kappa_i$  on  $(0, 1)$ . Using these facts, we have

$$\begin{aligned}
P(\kappa_i < \epsilon | X_i) &\leq \frac{\int_0^\epsilon \exp\left(-\frac{\kappa_i X_i^2}{2}\right) \kappa_i^{a-1/2} (1 - \kappa_i)^{b_n-1} d\kappa_i}{\int_\epsilon^1 \exp\left(-\frac{\kappa_i X_i^2}{2}\right) \kappa_i^{a-1/2} (1 - \kappa_i)^{b_n-1} d\kappa_i} \\
&\leq \frac{e^{X_i^2/2} \int_0^\epsilon \kappa_i^{a-1/2} (1 - \kappa_i)^{b_n-1} d\kappa_i}{\int_\epsilon^1 \kappa_i^{a-1/2} (1 - \kappa_i)^{b_n-1} d\kappa_i} \\
&\leq \frac{e^{X_i^2/2} (1 - \epsilon)^{b_n-1} \int_0^\epsilon \kappa_i^{a-1/2} d\kappa_i}{\epsilon^{a-1/2} \int_\epsilon^1 (1 - \kappa_i)^{b_n-1} d\kappa_i} \\
&= \frac{e^{X_i^2/2} (1 - \epsilon)^{b_n-1} \left(a + \frac{1}{2}\right)^{-1} \epsilon^{a+1/2}}{b_n^{-1} \epsilon^{a-1/2} (1 - \epsilon)^b} \\
&= e^{X_i^2/2} \frac{b_n \epsilon}{(a + 1/2) (1 - \epsilon)}.
\end{aligned}$$

□

*Proof of Theorem 3.* First, note that since  $b_n \in (0, 1)$ ,  $(1 - \kappa_i)^{b_n-1}$  is increasing in  $\kappa_i$  on  $(0, 1)$ . Therefore, letting  $C$  denote the normalizing constant that depends on  $X_i$ , we have

$$\begin{aligned}
\int_0^\eta \pi(\kappa_i | X_i) d\kappa_i &= C \int_0^\eta \exp\left(-\frac{\kappa_i X_i^2}{2}\right) \kappa_i^{a-1/2} (1 - \kappa_i)^{b_n-1} d\kappa_i \\
&\geq C \int_0^{\eta^\delta} \exp\left(-\frac{\kappa_i X_i^2}{2}\right) \kappa_i^{a-1/2} (1 - \kappa_i)^{b_n-1} d\kappa_i
\end{aligned}$$

$$\begin{aligned}
&\geq C \exp\left(-\frac{\eta\delta}{2}X_i^2\right) \int_0^{\eta\delta} \kappa_i^{a-1/2} d\kappa_i \\
&= C \exp\left(-\frac{\eta\delta}{2}X_i^2\right) \left(a + \frac{1}{2}\right)^{-1} (\eta\delta)^{a+\frac{1}{2}}.
\end{aligned} \tag{36}$$

Also, since  $a \in (\frac{1}{2}, \infty)$ ,  $\kappa_i^{a-1/2}$  is increasing in  $\kappa_i$  on  $(0, 1)$ .

$$\begin{aligned}
\int_{\eta}^1 \pi(\kappa_i|X_i) d\kappa_i &= C \int_{\eta}^1 \exp\left(-\frac{\kappa_i X_i^2}{2}\right) \kappa_i^{a-1/2} (1-\kappa_i)^{b_n-1} d\kappa_i \\
&\leq C \exp\left(-\frac{\eta X_i^2}{2}\right) \int_{\eta}^1 \kappa_i^{a-1/2} (1-\kappa_i)^{b_n-1} d\kappa_i \\
&\leq C \exp\left(-\frac{\eta X_i^2}{2}\right) \int_{\eta}^1 (1-\kappa_i)^{b_n-1} d\kappa_i \\
&= C \exp\left(-\frac{\eta X_i^2}{2}\right) b_n^{-1} (1-\eta)^{b_n}.
\end{aligned} \tag{37}$$

Combining (36) and (37), we have

$$\begin{aligned}
P(\kappa_i > \eta|X_i) &\leq \frac{\int_{\eta}^1 \pi(\kappa_i|X_i) d\kappa_i}{\int_0^{\eta} \pi(\kappa_i|X_i) d\kappa_i} \\
&\leq \frac{\left(a + \frac{1}{2}\right) (1-\eta)^{b_n}}{b_n (\eta\delta)^{a+\frac{1}{2}}} \exp\left(-\frac{\eta(1-\delta)}{2}X_i^2\right).
\end{aligned}$$

□

## B Proofs for Section 3.2

*Proof of Lemma 1.* It is enough to show that the second term on the left-hand side in (14) satisfies

$$d_n \int_1^{d_n^2} \frac{\pi(u)}{\sqrt{u}} du \gtrsim s_n. \tag{38}$$

We utilize the prior formulation in (5), so that the prior on the scale term is

$$\pi(u) \propto u^{a-1} (1+u)^{-(a+b)}.$$



Then for any  $a \in (\frac{1}{2}, \infty)$ , we have

$$\begin{aligned}
d_n \int_1^{d_n^2} \frac{\pi(u)}{\sqrt{u}} du &= d_n \int_1^{d_n^2} u^{a-3/2} (1+u)^{-(a+b)} du \\
&\gtrsim (1+d_n^2)^{-(a+b)} d_n^{2a} \\
&= (1+d_n^2)^{-(1+b)} \left( \frac{d_n^2}{1+d_n^2} \right)^{a-1} d_n^2 \quad (39)
\end{aligned}$$

Since  $d_n^2 = \log\left(\frac{n}{q_n}\right) \rightarrow \infty$  as  $n \rightarrow \infty$  and  $b = o(1)$  by assumption, we have  $\left(\frac{d_n^2}{1+d_n^2}\right)^{a-1} \sim 1$  and  $(1+d_n^2)^{-(1+b)} \sim (1+d_n^2)^{-1}$  for large  $n$ . Additionally, from the inequality,  $\log(1+x) \leq \sqrt{x}$  for  $x \geq 0$ , we have  $(1+x)^{-1} \geq \exp(-\sqrt{x})$  for  $x \geq 0$ . Combining these with (39), we have

$$\begin{aligned}
d_n \int_1^{d_n^2} \frac{\pi(u)}{\sqrt{u}} du &\gtrsim d_n^2 (1+d_n^2)^{-1} \\
&\geq d_n^2 \exp(-d_n) \\
&\geq d_n^2 \exp(-d_n^2) \quad (\text{for large } n) \\
&= \log\left(\frac{n}{q_n}\right) \frac{q_n}{n} \\
&= s_n,
\end{aligned}$$

and thus (38) holds for any  $a \in (\frac{1}{2}, \infty)$  and  $b = o(1)$ .  $\square$

Before proving Theorems 4 and 5, we first state two lemmas. For both Lemmas 2 and 3, we denote  $T(x) = \{\mathbb{E}(1-\kappa)|x\}x$  as the posterior mean under (9) for a single observation  $x$ , where  $\kappa = \frac{1}{1+\lambda\xi}$ . Our arguments follow closely those of van der Pas et al. [27], Datta and Ghosh [12], and Ghosh and Chakrabarti [16], except that their arguments rely on controlling the rate of decay of tuning parameter  $\tau$  or an empirical Bayes estimator  $\hat{\tau}$ . In our case, since we are dealing with a fully Bayesian model, the degree of posterior contraction is instead controlled by the positive sequence of hyperparameters  $b_n$  in (9).

**Lemma 2.** *Let  $T(x)$  be the posterior mean under (9) for a single observation  $x$  drawn from  $N(\theta, 1)$ . Suppose we have constants  $\eta \in (0, \frac{1}{2})$ ,  $\delta \in (0, 1)$ ,  $a \in (\frac{1}{2}, \infty)$ , and  $b_n \in (0, 1)$ , where  $b_n \rightarrow 0$  as  $n \rightarrow \infty$ . Then for any  $d > 2$  and fixed  $n$ ,  $|T(x) - x|$  can be bounded above by a real-valued function  $h_n(x)$ , depending on  $d$  and satisfying the following:*

For any  $\rho > d$ ,  $h_n(\cdot)$  satisfies

$$\lim_{n \rightarrow \infty} \sup_{|x| > \sqrt{\rho \log(\frac{1}{b_n})}} h_n(x) = 0. \quad (40)$$

*Proof of Lemma 2.* Fix  $\eta \in (0, 1)$ ,  $\delta \in (0, 1)$ . First observe that

$$\begin{aligned} |T(x) - x| &= |x \mathbb{E}(\kappa | x)| \\ &\leq |x \mathbb{E}(\kappa 1\{\kappa < \eta\})| + |x \mathbb{E}(\kappa 1\{\kappa > \eta\})|. \end{aligned} \quad (41)$$

We consider the two terms in (41) separately. From (7) and the fact that  $(1 - \kappa)^{b_n - 1}$  is increasing in  $\kappa \in (0, 1)$  when  $b_n \in (0, 1)$ , we have

$$\begin{aligned} |x \mathbb{E}(\kappa 1\{\kappa < \eta\})| &= \left| x \frac{\int_0^\eta \kappa \cdot \kappa^{a-1/2} (1 - \kappa)^{b_n-1} e^{-\kappa x^2/2} d\kappa}{\int_0^1 \kappa^{a-1/2} (1 - \kappa)^{b_n-1} e^{-\kappa x^2/2} d\kappa} \right| \\ &\leq |x| \left| (1 - \eta)^{b_n-1} \frac{\int_0^\eta \kappa^{a+1/2} e^{-\kappa x^2/2} d\kappa}{\int_0^1 \kappa^{a-1/2} e^{-\kappa x^2/2} d\kappa} \right| \\ &= (1 - \eta)^{b_n-1} \left| \frac{\int_0^{\eta x^2} \left(\frac{t}{x^2}\right)^{a+1/2} e^{-t/2} dt}{\int_0^{x^2} \left(\frac{t}{x^2}\right)^{a-1/2} e^{-t/2} dt} \right| |x| \\ &= (1 - \eta)^{b_n-1} \left| \frac{1}{x^2} \frac{\int_0^{\eta x^2} t^{a+1/2} e^{-t/2} dt}{\int_0^{x^2} t^{a-1/2} e^{-t/2} dt} \right| |x| \\ &\leq (1 - \eta)^{b_n-1} \left| \frac{\int_0^\infty t^{a+1/2} e^{-t/2} dt}{\int_0^{x^2} t^{a-1/2} e^{-t/2} dt} \right| |x|^{-1} \\ &= C(n) \left[ \left| \int_0^{x^2} t^{a-1/2} e^{-t/2} dt \right| \right]^{-1} |x|^{-1} \\ &= h_1(x) \quad (\text{say}), \end{aligned} \quad (42)$$

where we use a change of variables  $t = \kappa x^2$  in the second equality, and  $C(n) = (1 - \eta)^{b_n-1} \left( \frac{\Gamma(1)\Gamma(a+3/2)}{\Gamma(a+5/2)} \right) = (1 - \eta)^{b_n-1} \left( a + \frac{3}{2} \right)^{-1}$ .

Next, we observe that since  $\kappa \in (0, 1)$ ,

$$\begin{aligned} |x \mathbb{E}(\kappa 1\{\kappa > \eta\})| &\leq |x P(\kappa > \eta | x)| \\ &\leq \frac{\left(a + \frac{1}{2}\right) (1 - \eta)^{b_n}}{b_n (\eta \delta)^{a+1/2}} |x| \exp\left(-\frac{\eta(1 - \delta)}{2} x^2\right) \\ &= h_2(x) \quad (\text{say}), \end{aligned} \quad (43)$$

where we use Theorem 3 for the second inequality.

Let  $h_n(x) = h_1(x) + h_2(x)$ . Combining (41)-(43), we have that for every  $x \in \mathbb{R}$  and fixed  $n$ ,

$$|T(x) - x| \leq h_n(x), \quad (44)$$

Observe from (42) that for fixed  $n$ ,  $h_1(x)$  is strictly decreasing in  $|x|$ . Therefore, we have that for any fixed  $n$  and  $\rho > 0$ ,

$$\sup_{|x| > \sqrt{\rho \log\left(\frac{1}{b_n}\right)}} h_1(x) \leq C(n) \left[ \left| \sqrt{\rho \log\left(\frac{1}{b_n}\right)} \int_0^{\rho \log\left(\frac{1}{b_n}\right)} t^{a-1/2} e^{-t/2} dt \right| \right]^{-1},$$

and since  $b_n \rightarrow 0$  as  $n \rightarrow \infty$ , this implies that

$$\lim_{n \rightarrow \infty} \sup_{|x| > \sqrt{\rho \log\left(\frac{1}{b_n}\right)}} h_1(x) = 0. \quad (45)$$

Next, observe that from (43) that for fixed  $n$ ,  $h_2(x)$  is eventually decreasing in  $|x|$  with a maximum when  $|x| = \frac{1}{\sqrt{\eta(1-\delta)}}$ . Therefore, for sufficiently large  $n$ , we have

$$\sup_{|x| > \sqrt{\rho \log\left(\frac{1}{b_n}\right)}} h_2(x) \leq h_2\left(\sqrt{\rho \log\left(\frac{1}{b_n}\right)}\right).$$

Letting  $K \equiv K(a, \eta, \delta) = \frac{(a+\frac{1}{2})}{(\eta\delta)^{a+1/2}}$ , we have from (43) and the fact that  $0 < b_n < 1$  for all  $n$  that

$$\begin{aligned} \lim_{n \rightarrow \infty} h_2\left(\sqrt{\rho \log\left(\frac{1}{b_n}\right)}\right) &= K \lim_{n \rightarrow \infty} \frac{(1-\eta)^{b_n}}{b_n} \sqrt{\rho \log\left(\frac{1}{b_n}\right)} e^{-\frac{\eta(1-\delta)}{2} \rho \log\left(\frac{1}{b_n}\right)} \\ &\leq K \lim_{n \rightarrow \infty} \frac{1}{b_n} \sqrt{\rho \log\left(\frac{1}{b_n}\right)} e^{\frac{\eta(1-\delta)}{2} \log(b_n^\rho)} \\ &= K \sqrt{\rho} \lim_{n \rightarrow \infty} (b_n)^{\frac{\eta(1-\delta)}{2} (\rho - \frac{2}{\eta(1-\delta)})} \sqrt{\log\left(\frac{1}{b_n}\right)} \\ &= \begin{cases} 0 & \text{if } \rho > \frac{2}{\eta(1-\delta)}, \\ \infty & \text{otherwise,} \end{cases} \end{aligned}$$

from which it follows that

$$\lim_{n \rightarrow \infty} \sup_{|x| > \sqrt{\rho \log\left(\frac{1}{b_n}\right)}} h_2(x) = \begin{cases} 0 & \text{if } \rho > \frac{2}{\eta(1-\delta)}, \\ \infty & \text{otherwise.} \end{cases} \quad (46)$$

Combining (45) and (46), we have for  $h_n(x) = h_1(x) + h_2(x)$  that

$$\lim_{n \rightarrow \infty} \sup_{|x| > \sqrt{\rho \log(\frac{1}{b_n})}} h_n(x) = \begin{cases} 0 & \text{if } \rho > \frac{2}{\eta(1-\delta)}, \\ \infty & \text{otherwise.} \end{cases} \quad (47)$$

Since  $\eta \in (0, 1)$ ,  $\delta \in (0, 1)$ , it is clear that any real number larger than 2 can be expressed in the form  $\frac{2}{\eta(1-\delta)}$ . For example, taking  $\eta = \frac{5}{6}$  and  $\delta = \frac{1}{5}$ , we obtain  $\frac{2}{\eta(1-\delta)} = 3$ . Hence, given any  $d > 2$ , choose  $0 < \eta, \delta < 1$  such that  $c = \frac{2}{\eta(1-\delta)}$ . Clearly,  $h_n(\cdot)$  depends on  $d$ . Following (44) and (47), we see that  $|T(x) - x|$  is uniformly bounded above by  $h_n(x)$  for all  $n$  and  $d > 2$  and that condition (40) is also satisfied when  $d > 2$ . This completes the proof.  $\square$

**Remark:** Under the conditions of Lemma 2, we see that for any fixed  $n$ ,

$$\lim_{|x| \rightarrow \infty} |T(x) - x| = 0. \quad (48)$$

Equation (48) shows that for the IGG prior, large observations almost remain unshrunk no matter what the sample size  $n$  is. This is critical to its ability to properly identify signals in our data. We now present our second lemma which bounds the posterior variance.

**Lemma 3.** *Let  $T(x_i)$  be the posterior mean under (9). Then for a single observation  $x \sim N(\theta, 1)$ , the posterior variance  $\text{Var}(\theta|x)$  can be bounded above by*

$$\text{Var}(\theta|x) \leq 1 - (T(x) - x)^2 + x^2, \quad (49)$$

and

$$\text{Var}(\theta|x) \leq 1 - T(x)^2 + x^2. \quad (50)$$

*Proof of Lemma 3.* We first prove (49). By the law of the iterated variance and the fact that  $\theta|\kappa, x \sim N((1 - \kappa)x, 1 - \kappa)$ , we have

$$\begin{aligned} \text{Var}(\theta|x) &= \mathbb{E}[\text{Var}(\theta|\kappa, x)] + \text{Var}[\mathbb{E}(\theta|\kappa, x)] \\ &= \mathbb{E}(1 - \kappa|x) + \text{Var}[(1 - \kappa)x|x] \\ &= \mathbb{E}(1 - \kappa|x) + x^2 \text{Var}(\kappa|x) \\ &= \mathbb{E}[(1 - \kappa)x + x^2 \mathbb{E}(\kappa^2|x) - x^2 [\mathbb{E}(\kappa|x)]^2]. \end{aligned}$$

Since  $x - T(x) = x\mathbb{E}(\kappa|x)$ , we rewrite the above as

$$\text{Var}(\theta|x) = \frac{T(x)}{x} - (T(x) - x)^2 + x^2 \frac{\int_0^1 \kappa^{a+3/2} (1 - \kappa)^{b_n-1} e^{-\kappa x^2/2} dx}{\int_0^1 \kappa^{a+1/2} (1 - \kappa)^{b_n-1} e^{-\kappa x^2/2} dx}$$

$$\leq 1 - (T(x) - x)^2 + x^2,$$

where the inequality follows from the fact that  $\kappa \in (0, 1)$ , so  $\kappa^{a+\frac{3}{2}} \leq \kappa^{a+\frac{1}{2}}$  for all  $a \in \mathbb{R}$ .

Next, we show that (50) holds. We may alternatively represent  $\text{Var}(\theta|x)$  as

$$\begin{aligned} \text{Var}(\theta|x) &= \mathbb{E}(1 - \kappa|x) + x^2 \mathbb{E}[(1 - \kappa)^2|x] - x^2 \mathbb{E}^2[(1 - \kappa)|x] \\ &= \frac{T(x)}{x} - T(x)^2 + x^2 \frac{\int_0^1 \kappa^{a+1/2} (1 - \kappa)^{b_n+1} e^{-\kappa x^2/2} dx}{\int_0^1 \kappa^{a+1/2} (1 - \kappa)^{b_n-1} e^{-\kappa x^2/2} dx} \\ &\leq 1 - T(x)^2 + x^2, \end{aligned}$$

where the final inequality holds because  $(1 - \kappa)^{b_n+1} \leq (1 - \kappa)^{b_n-1}$  for all  $b_n \in \mathbb{R}$  when  $\kappa \in (0, 1)$ .  $\square$

Lemmas 2 and 3 are crucial in proving Theorems 4 and 5, which provide asymptotic upper bounds on the mean squared error (MSE) for the posterior mean under the  $\text{IGG}_n$  prior (9) and the posterior variance under (9). These theorems will ultimately allow us to provide sufficient conditions under which the posterior mean and posterior distribution under the  $\text{IGG}_n$  prior contract at minimax rates.

*Proof of Theorem 4.* Define  $\tilde{q}_n = \#\{i : \theta_{0i} \neq 0\}$ . We split the MSE,

$$\mathbb{E}_{\theta_0} \|T(\mathbf{X}) - \theta_0\|^2 = \sum_{i=1}^n \mathbb{E}_{\theta_{0i}} (T(X_i) - \theta_{0i})^2$$

as

$$\sum_{i=1}^n \mathbb{E}_{\theta_{0i}} (T(X_i) - \theta_{0i})^2 = \sum_{i:\theta_{0i} \neq 0} \mathbb{E}_{\theta_{0i}} (T(X_i) - \theta_{0i})^2 + \sum_{i:\theta_{0i}=0} \mathbb{E}_{\theta_{0i}} (T(X_i) - \theta_{0i})^2. \quad (51)$$

We consider the nonzero means and the zero means separately.

*Nonzero means:* For  $\theta_{0i} \neq 0$ , using the Cauchy-Schwartz inequality and the fact that  $\mathbb{E}_{\theta_{0i}}(X_i - \theta_{0i})^2 = 1$ , we get

$$\begin{aligned} \mathbb{E}_{\theta_{0i}} (T(X_i) - \theta_i)^2 &= \mathbb{E}_{\theta_{0i}} (T(X_i) - X_i + X_i - \theta_i)^2 \\ &= \mathbb{E}_{\theta_{0i}} (T(X_i) - X_i)^2 + \mathbb{E}_{\theta_{0i}} (X_i - \theta_{0i})^2 + 2\mathbb{E}_{\theta_{0i}} (T(X_i) - X_i)(X_i - \theta_{0i}) \\ &\leq \mathbb{E}_{\theta_{0i}} (T(X_i) - X_i)^2 + 1 + 2\sqrt{\mathbb{E}_{\theta_{0i}} (T(X_i) - X_i)^2} \sqrt{\mathbb{E}_{\theta_{0i}} (X_i - \theta_{0i})^2} \end{aligned}$$

$$= \left[ \sqrt{\mathbb{E}_{\theta_{0i}}(T(X_i) - X_i)^2 + 1} \right]^2. \quad (52)$$

We now define

$$\zeta_n = \sqrt{2 \log \left( \frac{1}{b_n} \right)}. \quad (53)$$

Let us fix any  $d > 2$  and choose any  $\rho > 2$ . Then, using Lemma 2, there exists a non-negative real-valued function  $h_n(\cdot)$ , depending on  $d$  such that

$$|T_n(x) - x| \leq h_n(x) \text{ for all } x \in \mathbb{R}, \quad (54)$$

and

$$\lim_{n \rightarrow \infty} \sup_{|x| > \rho \zeta_n} h_n(x) = 0. \quad (55)$$

Using the fact that  $(T(X_i) - X_i)^2 \leq X_i^2$ , together with (55), we obtain

$$\begin{aligned} \mathbb{E}_{\theta_{0i}}(T(X_i) - X_i)^2 &= \mathbb{E}_{\theta_{0i}}[(T(X_i) - X_i)^2 1\{|X_i| \leq \rho \zeta_n\}] \\ &\quad + \mathbb{E}_{\theta_{0i}}[T(X_i) - X_i)^2 1\{|X_i| > \rho \zeta_n\}] \\ &\leq \rho^2 \zeta_n^2 + \left( \sup_{|x| > \rho \zeta_n} h_n(x) \right)^2. \end{aligned} \quad (56)$$

Using (55) and the fact that  $\zeta_n \rightarrow \infty$  as  $n \rightarrow \infty$  by (53), it follows that

$$\left( \sup_{|x| > \rho \zeta_n} h_n(x) \right)^2 = o(\zeta_n^2) \text{ as } n \rightarrow \infty. \quad (57)$$

By combining (56) and (57), we get

$$\mathbb{E}_{\theta_{0i}}(T(X_i) - X_i)^2 \leq \rho^2 \zeta_n^2 (1 + o(1)) \text{ as } n \rightarrow \infty. \quad (58)$$

Noting that (58) holds uniformly for any  $i$  such that  $\theta_{0i} \neq 0$ , we combine (52), (53), and (58) to conclude that

$$\sum_{i: \theta_{0i} \neq 0} \mathbb{E}_{\theta_{0i}}(T(X_i) - \theta_{0i})^2 \lesssim \tilde{q}_n \log \left( \frac{1}{b_n} \right), \text{ as } n \rightarrow \infty, \quad (59)$$

*Zero means:* For  $\theta_{0i} = 0$ , the corresponding MSE can be split as follows:

$$\mathbb{E}_0 T(X_i)^2 = \mathbb{E}_0 [T(X_i)^2 1\{|X_i| \leq \zeta_n\}] + \mathbb{E}_0 [T(X_i)^2 1\{|X_i| > \zeta_n\}], \quad (60)$$

where  $\zeta_n$  is as in (53). Using Theorem 1, we have

$$\begin{aligned}
\mathbb{E}_0[T(X_i)^2 1\{|X_i| \leq \zeta_n\}] &\leq \left(\frac{b_n}{a + b_n + 1/2}\right)^2 \int_{-\zeta_n}^{\zeta_n} x^2 e^{x^2/2} dx \\
&\leq \frac{b_n^2}{a^2} \int_{-\zeta_n}^{\zeta_n} x^2 e^{x^2/2} dx \\
&= \frac{2b_n^2}{a^2} \int_0^{\zeta_n} x^2 e^{x^2/2} dx \\
&\leq \frac{2b_n^2}{a} (\zeta_n e^{\zeta_n^2/2}) \\
&\lesssim b_n \sqrt{\log\left(\frac{1}{b_n}\right)},
\end{aligned} \tag{61}$$

where we use the integration by parts for the third inequality.

Now, using the fact that  $|T(x)| \leq |x|$  for all  $x \in \mathbb{R}$ ,

$$\begin{aligned}
\mathbb{E}_0[T(X_i)^2 1\{|X_i| > \zeta_n\}] &\leq 2 \int_{\zeta_n}^{\infty} x^2 \phi(x) dx \\
&= 2[\zeta_n \phi(\zeta_n) + 1 - \Phi(\zeta_n)] \\
&\leq 2\zeta_n \phi(\zeta_n) + \frac{2\phi(\zeta_n)}{\zeta_n} \\
&= \sqrt{\frac{2}{\pi}} \zeta_n (e^{-\zeta_n^2/2} + o(1)) \\
&\lesssim b_n \sqrt{\log\left(\frac{1}{b_n}\right)},
\end{aligned} \tag{62}$$

where we used the identity  $x^2 \phi(x) = \phi(x) - \frac{d}{dx}[x\phi(x)]$  for the first equality and Mill's ratio,  $1 - \Phi(x) \leq \frac{\phi(x)}{x}$  for all  $x > 0$ , in the second inequality. Combining (61)-(62), we have that

$$\sum_{i:\theta_{0i}=0} \mathbb{E}_{\theta_{0i}} T(X_i)^2 \lesssim (n - \tilde{q}_n) b_n \sqrt{\log\left(\frac{1}{b_n}\right)}. \tag{63}$$

From (51), (59) and (63), it immediately follows that

$$\begin{aligned}
\mathbb{E}||T(\mathbf{X}) - \boldsymbol{\theta}_0||^2 &= \sum_{i=1}^n \mathbb{E}_{\theta_{0i}} (T(X_i) - \theta_{0i})^2 \\
&\lesssim \tilde{q}_n \log\left(\frac{1}{b_n}\right) + (n - \tilde{q}_n) b_n \sqrt{\log\left(\frac{1}{b_n}\right)}.
\end{aligned}$$

The required result now follows by observing that  $\tilde{q}_n \leq q_n$  and  $q_n = o(n)$  and then taking the supremum over all  $\boldsymbol{\theta}_0 \in \ell_0[q_n]$ . This completes the proof of Theorem 4.  $\square$

*Proof of Theorem 5.* Define  $\tilde{q}_n = \#\{i : \theta_{0i} \neq 0\}$ . We decompose the total variance as

$$\mathbb{E}_{\boldsymbol{\theta}_0} \sum_{i=1}^n \text{Var}(\theta_{0i}|X_i) = \sum_{i:\theta_{0i} \neq 0} \mathbb{E}_{\theta_{0i}} \text{Var}(\theta_{0i}|X_i) + \sum_{i:\theta_{0i}=0} \mathbb{E}_{\theta_{0i}} \text{Var}(\theta_{0i}|X_i), \quad (64)$$

and consider the nonzero means and zero means separately.

*Nonzero means:* For  $\theta_{0i} \neq 0$ , we have

$$\begin{aligned} \mathbb{E}_{\theta_{0i}} \text{Var}(\theta_{0i}|X_i) &\leq \mathbb{E}_{\theta_{0i}} [1 - (T(X_i) - X_i)^2 + X_i^2] \\ &\leq 2 + \mathbb{E}_{\theta_{0i}} (T(X_i) - X_i)^2 \\ &\lesssim \log \left( \frac{1}{b_n} \right), \end{aligned} \quad (65)$$

where the first inequality follows from (49) in Lemma 3 and the last one follows from (58).

*Zero means:* For  $\theta_{0i} = 0$ , we have

$$\begin{aligned} \mathbb{E}_0 \text{Var}(\theta_{0i}|X_i) &\leq \mathbb{E}_0 [1 - T(X_i)^2 + X_i^2] \\ &\leq 2 + \mathbb{E}_0 T(X_i)^2 \\ &\lesssim b_n \sqrt{\log \left( \frac{1}{b_n} \right)}, \end{aligned} \quad (66)$$

where the first inequality follows from (50) in Lemma 3 and the last one follows from (60)-(62). Combining (64)-(66), we get

$$\mathbb{E}_{\boldsymbol{\theta}_0} \text{Var}(\theta_{0i}|X_i) \lesssim \tilde{q}_n \log \left( \frac{1}{b_n} \right) + (n - \tilde{q}_n) b_n \sqrt{\log \left( \frac{1}{b_n} \right)}.$$

The required result now follows by observing that  $\tilde{q}_n \leq q_n$  and  $q_n = o(n)$  and then taking the supremum over all  $\boldsymbol{\theta}_0 \in \ell_0[q_n]$ . This completes the proof of Theorem 5.  $\square$



## C Proofs for Section 3.3

*Proof of Theorem 7.* Using the beta prime representation of the IGG prior, we have

$$\pi(\theta) = \frac{1}{(2\pi)^{\frac{1}{2}} B(a, b)} \int_0^\infty \exp\left(-\frac{\theta^2}{2u}\right) u^{b-\frac{3}{2}} (1+u)^{-a-b} du,$$

where  $B(a, b)$  denotes the beta function. Under the transformation of variables,  $z = \frac{\theta^2}{2u}$ , we have

$$\pi(\theta) = \frac{2^{a+\frac{1}{2}}}{(2\pi)^{\frac{1}{2}} B(a, b)} (\theta^2)^{b-\frac{1}{2}} \int_0^\infty \exp(-z) z^{a-\frac{1}{2}} (\theta^2 + 2z)^{-a-b} dz. \quad (67)$$

Now define the set  $A_\epsilon = \{\theta : |\theta| \leq \epsilon\}$ . Then from (67), and for  $0 < \epsilon < 1$ , we have

$$\begin{aligned} \nu(A_\epsilon) &= P(|\theta| \leq \epsilon) \\ &= \frac{2^{a+\frac{1}{2}} \int_0^\infty \exp(-z) z^{a-\frac{1}{2}} \left( \int_{|\theta| \leq \epsilon} (\theta^2)^{2b-\frac{1}{2}} (\theta^2 + 2z)^{-b} d\theta \right) dz}{(2\pi)^{\frac{1}{2}} B(a, b)} \\ &\geq \frac{2^{a+\frac{1}{2}} \int_0^\infty \exp(-z) z^{a-\frac{1}{2}} (2z+1)^{-a-b} \left( \int_{|\theta| \leq \epsilon} (\theta^2)^{b-\frac{1}{2}} d\theta \right) dz}{(2\pi)^{\frac{1}{2}} B(a, b)} \\ &\geq \frac{2^{a+\frac{1}{2}} 2^{-a-b} \int_0^\infty \exp(-z) z^{a-\frac{1}{2}} (1+z)^{-a-b} \left( \int_0^\epsilon (\theta^2)^{b-\frac{1}{2}} d\theta \right) dz}{(2\pi)^{\frac{1}{2}} B(a, b)} \\ &= \frac{\epsilon^{2b}}{2^b b B(a, b) \pi^{1/2}} \int_0^\infty \exp(-z) z^{a-\frac{1}{2}} (1+z)^{-a-b} dz. \end{aligned} \quad (68)$$

To bound the integral term in (68), note that

$$\begin{aligned} \int_0^\infty \exp(-z) z^{a-\frac{1}{2}} (1+z)^{-a-b} dz &\geq \int_0^1 \exp(-z) z^{a-\frac{1}{2}} (1+z)^{-a-b} dz \\ &\geq e^{-1} 2^{-a-b} \left(a + \frac{1}{2}\right)^{-1}. \end{aligned} \quad (69)$$

Therefore, combining (68) and (69), we have

$$\nu(A_\epsilon) \geq \frac{\epsilon^{2b}}{2^b b B(a, b) \pi^{1/2}} e^{-1} 2^{-a-b} \left(a + \frac{1}{2}\right)^{-1}$$

$$\begin{aligned}
&= \frac{\epsilon^{2b}\Gamma(a+b)}{2^b\Gamma(a)\Gamma(b+1)\pi^{1/2}} e^{-1} 2^{-a-b} \left(a + \frac{1}{2}\right)^{-1} \\
&\geq \frac{\epsilon^{2b}\Gamma(a)}{\Gamma(a)\Gamma(2)\Gamma(\frac{1}{2})} e^{-1} 2^{-a-2b} \left(a + \frac{1}{2}\right)^{-1} \\
&\geq (\epsilon^2)^b (\pi)^{-1/2} e^{-1} 2^{-a-2} \left(a + \frac{1}{2}\right)^{-1}, \tag{70}
\end{aligned}$$

where we use the fact that  $0 < b < 1$  for the last two inequalities.

Following Clarke and Barron [11], the optimal rate of convergence comes from setting  $\epsilon_n = 1/n$ , which reflects the ideal case of independent samples  $y_1, \dots, y_n$ . We therefore apply Proposition 3, substituting in  $\epsilon = 1/n$  and  $b = 1/n$  and invoking the lower bound for  $\nu(A_\epsilon)$  found in (70). This ultimately gives us an upper bound on the Cesàro-average risk as

$$\begin{aligned}
R_n &\leq \frac{1}{n} - \frac{1}{n} \log \left[ \left(\frac{1}{n}\right)^{\frac{2}{n}} \pi^{-1/2} e^{-1} 2^{-a-2} \left(a + \frac{1}{2}\right)^{-1} \right] \\
&= \frac{1}{n} \left[ 2 + \log(\sqrt{\pi}) + (a+2)\log(2) + \log\left(a + \frac{1}{2}\right) \right] + \frac{2\log n}{n^2},
\end{aligned}$$

when  $\theta_0 = 0$ . □

## D Proofs for Section 4

To establish conditions for (29) to hold, we must first find lower and upper bounds on the Type I and Type II error probabilities,  $t_{1i}$  and  $t_{2i}$  respectively, for rule (28). These error probabilities are given respectively by

$$\begin{aligned}
t_{1i} &= P \left[ \mathbb{E}(1 - \kappa_i | X_i) > \frac{1}{2} \middle| H_{0i} \text{ is true} \right], \\
t_{2i} &= P \left[ \mathbb{E}(1 - \kappa_i | X_i) \leq \frac{1}{2} \middle| H_{1i} \text{ is true} \right]. \tag{71}
\end{aligned}$$

To this end, we first prove the following lemmas, Lemma 4-7 which give upper and lower bounds for  $t_{1i}$  and  $t_{2i}$  in (71). Our proof methods follow those of Datta and Ghosh [12], [17], and Ghosh and Chakrabarti [16], except our arguments rely on control of the sequence of hyperparameters  $b_n$ , rather than on specifying a rate or an estimate for a global parameter  $\tau$ , as in the global-local (3) framework.

**Lemma 4.** Suppose that  $X_1, \dots, X_n$  are i.i.d. observations having distribution (22) where the sequence of vectors  $(\psi^2, p)$  satisfies Assumption 1. Suppose we wish to test (23) using the classification rule (28). Then for all  $n$ , an upper bound for the probability of a Type I error for the  $i$ th test is given by

$$t_{1i} \leq \frac{2b_n}{\sqrt{\pi}(a + b_n + 1/2)} \left[ \log \left( \frac{a + b_n + 1/2}{2b_n} \right) \right]^{-1/2}.$$

*Proof of Lemma 4.* By Theorem 1, the event  $\{\mathbb{E}(1 - \kappa_i | X_i) > \frac{1}{2}\}$  implies the event

$$\begin{aligned} & \left\{ e^{X_i^2/2} \left( \frac{b_n}{a + b_n + 1/2} \right) > \frac{1}{2} \right\} \\ \Leftrightarrow & \left\{ X_i^2 > 2 \log \left( \frac{a + b_n + 1/2}{2b_n} \right) \right\}. \end{aligned}$$

Therefore, noting that under  $H_{0i}$ ,  $X_i \sim N(0, 1)$  and using Mill's ratio, i.e.  $P(|Z| > x) \leq \frac{2\phi(x)}{x}$ , we have

$$\begin{aligned} t_{1i} & \leq P \left( X_i^2 > 2 \log \left( \frac{a + b_n + 1/2}{2b_n} \right) \middle| H_{0i} \text{ is true} \right) \\ & = P \left( |Z| > \sqrt{2 \log \left( \frac{a + b_n + 1/2}{2b_n} \right)} \right) \\ & \leq \frac{2\phi \left( \sqrt{2 \log \left( \frac{a + b_n + 1/2}{2b_n} \right)} \right)}{\sqrt{2 \log \left( \frac{a + b_n + 1/2}{2b_n} \right)}} \\ & = \frac{2b_n}{\sqrt{\pi}(a + b_n + 1/2)} \left[ \log \left( \frac{a + b_n + 1/2}{2b_n} \right) \right]^{-1/2}. \end{aligned}$$

□

**Lemma 5.** Suppose that  $X_1, \dots, X_n$  are i.i.d. observations having distribution (22) where the sequence of vectors  $(\psi^2, p)$  satisfies Assumption 1. Suppose we wish to test (23) using the classification rule (28). Suppose further that  $a \in (\frac{1}{2}, \infty)$  and  $b_n \in (0, 1)$ , with  $b_n \rightarrow 0$  as  $n \rightarrow \infty$ . Then for

any  $\eta \in (0, \frac{1}{2})$ ,  $\delta \in (0, 1)$ , and sufficiently large  $n$ , a lower bound for the probability of a Type I error for the  $i$ th test is given by

$$t_{1i} \geq 1 - \Phi \left( \sqrt{\frac{2}{\eta(1-\delta)} \left[ \log \left( \frac{\left(a + \frac{1}{2}\right) (1-\eta)^{b_n}}{b_n(\eta\delta)^{a+\frac{1}{2}}} \right) \right]} \right).$$

*Proof of Lemma 5.* By definition, the probability of a Type I error for the  $i$ th decision is given by

$$t_{1i} = P \left[ \mathbb{E}(1 - \kappa_i | X_i) > \frac{1}{2} \mid H_{0i} \text{ is true} \right].$$

We have by Theorem 3 that

$$\mathbb{E}(\kappa_i | X_i) \leq \eta + \frac{\left(a + \frac{1}{2}\right) (1-\eta)^{b_n}}{b_n(\eta\delta)^{a+\frac{1}{2}}} \exp \left( -\frac{\eta(1-\delta)}{2} X_i^2 \right),$$

and so it follows that

$$\left\{ \mathbb{E}(1 - \kappa_i | X_i) > \frac{1}{2} \right\} \supseteq \left\{ \frac{\left(a + \frac{1}{2}\right) (1-\eta)^{b_n}}{b_n(\eta\delta)^{a+\frac{1}{2}}} \exp \left( -\frac{\eta(1-\delta)}{2} X_i^2 \right) < \frac{1}{2} - \eta \right\}.$$

Thus, using the definition of  $t_{1i}$  and the above and noting that under  $H_{0i}$ ,  $X_i \sim N(0, 1)$ , as  $n \rightarrow \infty$ ,

$$\begin{aligned} t_{1i} &\geq P \left( \frac{\left(a + \frac{1}{2}\right) (1-\eta)^{b_n}}{b_n(\eta\delta)^{a+\frac{1}{2}}} \exp \left( -\frac{\eta(1-\delta)}{2} X_i^2 \right) < \frac{1}{2} - \eta \mid H_{0i} \text{ is true} \right) \\ &= P \left( X_i^2 > \frac{2}{\eta(1-\delta)} \left[ \log \left( \frac{\left(a + \frac{1}{2}\right) (1-\eta)^{b_n}}{b_n(\eta\delta)^{a+\frac{1}{2}} \left(\frac{1}{2} - \eta\right)} \right) \right] \right) \\ &= 2P \left( Z > \sqrt{\frac{2}{\eta(1-\delta)} \left[ \log \left( \frac{\left(a + \frac{1}{2}\right) (1-\eta)^{b_n}}{b_n(\eta\delta)^{a+\frac{1}{2}} \left(\frac{1}{2} - \eta\right)} \right) \right]} \right) \\ &= 2 \left( 1 - \Phi \left( \sqrt{\frac{2}{\eta(1-\delta)} \left[ \log \left( \frac{\left(a + \frac{1}{2}\right) (1-\eta)^{b_n}}{b_n(\eta\delta)^{a+\frac{1}{2}} \left(\frac{1}{2} - \eta\right)} \right) \right]} \right) \right), \end{aligned}$$

where for the last inequality, we used the fact that  $b_n \rightarrow 0$  as  $n \rightarrow \infty$ , and the fact that  $\eta, \eta\delta \in (0, \frac{1}{2})$ , so that the  $\log(\cdot)$  term in final equality is greater than zero for sufficiently large  $n$ .  $\square$

**Lemma 6.** Suppose we have the same set-up as Lemma 4. Assume further that  $b_n \rightarrow 0$  in such a way that  $\lim_{n \rightarrow \infty} \frac{b_n^{1/4}}{p_n} \in (0, \infty)$ . Then for any  $\eta \in (0, \frac{1}{2})$ ,  $\delta \in (0, 1)$ , and sufficiently large  $n$ , an upper bound for the probability of a Type II error for the  $i$ th test is given by

$$t_{2i} \leq \left[ 2\Phi \left( \sqrt{\frac{C}{2\eta(1-\delta)}} \right) - 1 \right] (1 + o(1)),$$

where the  $o(1)$  terms tend to zero as  $n \rightarrow \infty$ .

*Proof of Lemma 6.* By definition, the probability of a Type II error is given by

$$t_{2i} = P \left( \mathbb{E}(1 - \kappa_i) \leq \frac{1}{2} \middle| H_{1i} \text{ is true} \right).$$

Fix  $\eta \in (0, \frac{1}{2})$  and  $\delta \in (0, 1)$ . Using the inequality,

$$\kappa_i \leq 1 \{ \eta < \kappa_i \leq 1 \} + \eta,$$

we obtain

$$\mathbb{E}(\kappa_i | X_i) \leq P(\kappa_i > \eta | X_i) + \eta.$$

Coupled with Theorem 3, we obtain that for sufficiently large  $n$ ,

$$\left\{ \mathbb{E}(\kappa_i | X_i) > \frac{1}{2} \right\} \subseteq \left\{ \frac{\left(a + \frac{1}{2}\right) (1 - \eta)^{b_n}}{b_n(\eta\delta)^{a+\frac{1}{2}}} \exp \left( -\frac{\eta(1-\delta)}{2} X_i^2 \right) > \frac{1}{2} - \eta \right\}.$$

Therefore,

$$\begin{aligned} t_{2i} &= P \left( \mathbb{E}(\kappa_i | X_i) > \frac{1}{2} \middle| H_{1i} \text{ is true} \right) \\ &\leq P \left( \frac{\left(a + \frac{1}{2}\right) (1 - \eta)^{b_n}}{b(\eta\delta)^{a+\frac{1}{2}}} \exp \left( -\frac{\eta(1-\delta)}{2} X_i^2 \right) > \frac{1}{2} - \eta \middle| H_{1i} \text{ is true} \right) \\ &= P \left( X_i^2 < \frac{2}{\eta(1-\delta)} \left\{ \log \left( \frac{a + \frac{1}{2}}{b_n(\eta\delta)^a} \right) - \log \left( \frac{\left(\frac{1}{2} - \eta\right) (\eta\delta)^{1/2}}{(1-\eta)^{b_n}} \right) \right\} \middle| H_{1i} \text{ is true} \right) \\ &= P \left( X_i^2 < \frac{2}{\eta(1-\delta)} \log \left( \frac{a}{b_n(\eta\delta)^a} \right) (1 + o(1)) \middle| H_{1i} \text{ is true} \right), \end{aligned} \quad (72)$$

where in the final equality, we used the fact that  $b_n \rightarrow 0$  as  $n \rightarrow \infty$ , so the second  $\log(\cdot)$  term in the second to last equality is a bounded quantity.

Note that under  $H_{1i}, X_i \sim N(0, 1 + \psi^2)$ . Therefore, by (72) and the fact that  $\lim_{n \rightarrow \infty} \frac{\psi_n^2}{1 + \psi_n^2} = 1$  (by the second condition of Assumption 1), we have

$$t_{2i} \leq P \left( |Z| < \sqrt{\frac{2}{\eta(1-\delta)}} \sqrt{\frac{\log(a(\eta\delta)^{-a}b_n^{-1})}{\psi^2}} (1 + o(1)) \right) \text{ as } n \rightarrow \infty. \quad (73)$$

By assumption,  $\lim_{n \rightarrow \infty} \frac{b_n^{1/4}}{p_n} \in (0, \infty)$ . This then implies that  $\lim_{n \rightarrow \infty} \frac{b_n^{7/8}}{p_n^2} = 0$ . Therefore, by the fourth condition of Assumption 1 and the fact that  $\psi^2 \rightarrow \infty$  as  $n \rightarrow \infty$ , we have

$$\begin{aligned} \frac{\log(a(\eta\delta)^{-a}b_n^{-1})}{\psi^2} &= \frac{\log(a(\eta\delta)^{-a}) + \log(b_n^{-1})}{\psi^2} \\ &= \left( \frac{\log(b_n^{-1/8})}{\psi^2} + \frac{\log(b_n^{-7/8})}{\psi^2} \right) (1 + o(1)) \\ &= \frac{\log(b_n^{-1/2})}{4\psi^2} (1 + o(1)) \\ &\rightarrow \frac{C}{4} \text{ as } n \rightarrow \infty. \end{aligned} \quad (74)$$

Thus, using (73) and (74), we have

$$\begin{aligned} t_{2i} &\leq P \left( |Z| < \sqrt{\frac{C}{2\eta(1-\delta)}} (1 + o(1)) \right) \text{ as } n \rightarrow \infty \\ &= P \left( |Z| < \sqrt{\frac{C}{2\eta(1-\delta)}} \right) (1 + o(1)) \text{ as } n \rightarrow \infty \\ &= 2 \left[ \Phi \left( \sqrt{\frac{C}{2\eta(1-\delta)}} \right) - 1 \right] (1 + o(1)) \text{ as } n \rightarrow \infty. \end{aligned}$$

□

**Lemma 7.** *Suppose we have the same set-up as Lemma 4. Then a lower bound for the probability of a Type II error for the  $i$ th test is given by*

$$t_{2i} \geq \left[ 2\Phi(\sqrt{C}) - 1 \right] (1 + o(1)) \text{ as } n \rightarrow \infty,$$

where the  $o(1)$  terms tend to zero as  $n \rightarrow \infty$ .

*Proof of Lemma 7.* By definition, the probability of a Type II error for the  $i$ th decision is given by

$$t_{2i} = P\left(\mathbb{E}(1 - \kappa_i) \leq \frac{1}{2} \middle| H_{1i} \text{ is true}\right).$$

For any  $n$ , we have by Theorem 1 that

$$\left\{e^{X_i^2/2} \left(\frac{b_n}{a + b_n + 1/2}\right) \leq \frac{1}{2}\right\} \subseteq \left\{\mathbb{E}(1 - \kappa_i | X_i) \leq \frac{1}{2}\right\}.$$

Therefore,

$$\begin{aligned} t_{2i} &= P\left(\mathbb{E}(1 - \kappa_i | X_i) \leq \frac{1}{2} \middle| H_{1i} \text{ is true}\right) \\ &\geq P\left(e^{X_i^2/2} \left(\frac{b_n}{a + b_n + 1/2}\right) \leq \frac{1}{2} \middle| H_{1i} \text{ is true}\right) \\ &= P\left(X_i^2 \leq 2 \log\left(\frac{a + b_n + 1/2}{2b_n}\right) \middle| H_{1i} \text{ is true}\right). \end{aligned} \quad (75)$$

Since  $X_i \sim N(0, 1 + \psi^2)$  under  $H_{1i}$ , we have by the second condition in Assumption 1 that  $\lim_{n \rightarrow \infty} \frac{\psi_n^2}{1 + \psi_n^2} \rightarrow 1$ . From (75) and the facts that  $a \in (\frac{1}{2}, \infty)$  and  $b_n \in (0, 1)$  for all  $n$  (so  $b_n^{-1} \geq b_n^{-1/2}$  for all  $n$ ), we have for sufficiently large  $n$ ,

$$\begin{aligned} t_{2i} &\geq P\left(|Z| \leq \sqrt{\frac{2 \log\left(\frac{a + b_n + 1/2}{2b_n}\right)}{\psi^2}}(1 + o(1)) \middle| \text{as } n \rightarrow \infty\right) \\ &\geq P\left(|Z| \leq \sqrt{\frac{\log\left(\frac{1}{2b_n}\right)}{\psi^2}}(1 + o(1)) \middle| \text{as } n \rightarrow \infty\right) \\ &\geq P\left(|Z| \leq \sqrt{\frac{\log(b_n^{-1/2}) + \log(1/2)}{\psi^2}}(1 + o(1)) \middle| \text{as } n \rightarrow \infty\right) \\ &= P(|Z| \leq \sqrt{C})(1 + o(1)) \text{ as } n \rightarrow \infty \\ &= 2[\Phi(\sqrt{C}) - 1](1 + o(1)) \text{ as } n \rightarrow \infty, \end{aligned}$$

where in the second to last equality, we used the assumption that  $\lim_{n \rightarrow \infty} \frac{b_n^{1/4}}{p_n} \in (0, \infty)$  and the second and fourth conditions from Assumption 1.  $\square$

*Proof of Theorem 8.* Since the  $\kappa_i$ 's,  $i = 1, \dots, n$  are *a posteriori* independent, the Type I and Type II error probabilities  $t_{1i}$  and  $t_{2i}$  are the same for every test  $i, i = 1, \dots, n$ . By Lemmas 4 and 5, for large enough  $n$ ,

$$\begin{aligned} & 2 \left( 1 - \Phi \left( \sqrt{\frac{2}{\eta(1-\delta)} \left[ \log \left( \frac{\left(a + \frac{1}{2}\right)(1-\eta)^{b_n}}{b_n(\eta\delta)^{a+\frac{1}{2}} \left(\frac{1}{2} - \eta\right)} \right) \right]} \right) \right) \leq t_{1i} \\ & \leq \frac{2b_n}{\sqrt{\pi}(a + b_n + 1/2)} \left[ \log \left( \frac{a + b_n + 1/2}{2b_n} \right) \right]^{-1/2}. \end{aligned}$$

Taking the limit as  $n \rightarrow \infty$  of all the terms above and using the sandwich theorem, we have

$$\lim_{n \rightarrow \infty} t_{1i} = 0 \quad (76)$$

for the  $i$ th test, under the assumptions on the hyperparameters  $a$  and  $b_n$ .

By Lemmas 6 and 7, for any  $\eta \in (0, \frac{1}{2})$  and  $\delta \in (0, 1)$ ,

$$\left[ 2\Phi(\sqrt{C}) - 1 \right] (1 + o(1)) \leq t_{2i} \leq \left[ 2\Phi \left( \sqrt{\frac{C}{2\eta(1-\delta)}} \right) - 1 \right] (1 + o(1)). \quad (77)$$

Therefore, we have by (76) and (77) that as  $n \rightarrow \infty$ , the asymptotic risk (24) of the classification rule (28),  $R_{IGG}$ , can be bounded as follows:

$$np(2\Phi(\sqrt{C}) - 1)(1 + o(1)) \leq R_{IGG} \leq np \left( 2\Phi \left( \sqrt{\frac{C}{2\eta(1-\delta)}} \right) - 1 \right) (1 + o(1)). \quad (78)$$

Therefore, from (26) and (78), we have as  $n \rightarrow \infty$ ,

$$1 \leq \liminf_{n \rightarrow \infty} \frac{R_{IGG}}{R_{Opt}^{BO}} \leq \limsup_{n \rightarrow \infty} \frac{R_{IGG}}{R_{Opt}^{BO}} \leq \frac{2\Phi \left( \sqrt{\frac{C}{2\eta(1-\delta)}} \right) - 1}{2\Phi(\sqrt{C}) - 1}. \quad (79)$$

Now, the supremum of  $\eta(1-\delta)$  over the grid  $(\eta, \delta) \in (0, \frac{1}{2}) \times (0, 1)$  is clearly  $\frac{1}{2}$ , and so the infimum of the numerator in the right-most term in (79) is therefore  $2\Phi(\sqrt{C}) - 1$ . Thus, one has that

$$1 \leq \liminf_{n \rightarrow \infty} \frac{R_{IGG}}{R_{Opt}^{BO}} \leq \limsup_{n \rightarrow \infty} \frac{R_{IGG}}{R_{Opt}^{BO}} \leq 1,$$

so classification rule (28) is ABOS, i.e.

$$\frac{R_{IGG}}{R_{Opt}^{BO}} \rightarrow 1 \text{ as } n \rightarrow \infty.$$

□



## References

- [1] Armagan, A., Clyde, M., and Dunson, D. B. (2011). Generalized beta mixtures of gaussians. In Shawe-taylor, J., Zemel, R., Bartlett, P., Pereira, F., and Weinberger, K., editors, *Advances in Neural Information Processing Systems 24*, pages 523–531.
- [2] Armagan, A., Dunson, D. B., and Lee, J. (2013). Generalized double pareto shrinkage. *Statistica Sinica*, 23 1:119–143.
- [3] Benjamini, Y. and Hochberg, Y. (1995). Controlling the false discovery rate: A practical and powerful approach to multiple testing. *Journal of the Royal Statistical Society. Series B (Methodological)*, 57(1):289–300.
- [4] Berger, J. (1980). A robust generalized bayes estimator and confidence region for a multivariate normal mean. *Ann. Statist.*, 8(4):716–761.
- [5] Bhadra, A., Datta, J., Polson, N. G., and Willard, B. (2017). The horseshoe+ estimator of ultra-sparse signals. *Bayesian Anal.*, 12(4):1105–1131.
- [6] Bhattacharya, A., Pati, D., Pillai, N. S., and Dunson, D. B. (2015). Dirichlet–laplace priors for optimal shrinkage. *Journal of the American Statistical Association*, 110(512):1479–1490. PMID: 27019543.
- [7] Bogdan, M., Chakrabarti, A., Frommlet, F., and Ghosh, J. K. (2011). Asymptotic bayes-optimality under sparsity of some multiple testing procedures. *Ann. Statist.*, 39(3):1551–1579.
- [8] Carvalho, C. M., Polson, N. G., and Scott, J. G. (2009). Handling sparsity via the horseshoe. In van Dyk, D. and Welling, M., editors, *Proceedings of the Twelfth International Conference on Artificial Intelligence and Statistics*, volume 5 of *Proceedings of Machine Learning Research*, pages 73–80, Hilton Clearwater Beach Resort, Clearwater Beach, Florida USA. PMLR.
- [9] Carvalho, C. M., Polson, N. G., and Scott, J. G. (2010). The horseshoe estimator for sparse signals. *Biometrika*, 97(2):465–480.
- [10] Castillo, I. and van der Vaart, A. (2012). Needles and straw in a haystack: Posterior concentration for possibly sparse sequences. *Ann. Statist.*, 40(4):2069–2101.

- [11] Clarke, B. S. and Barron, A. R. (1990). Information-theoretic asymptotics of bayes methods. *IEEE Transactions on Information Theory*, 36:453–471.
- [12] Datta, J. and Ghosh, J. K. (2013). Asymptotic properties of bayes risk for the horseshoe prior. *Bayesian Anal.*, 8(1):111–132.
- [13] Donoho, D. L., Johnstone, I. M., Hoch, J. C., and Stern, A. S. (1992). Maximum entropy and the nearly black object. *Journal of the Royal Statistical Society. Series B (Methodological)*, 54(1):41–81.
- [14] Efron, B. (2010). The future of indirect evidence. *Statist. Sci.*, 25(2):145–157.
- [15] Ghosal, S., Ghosh, J. K., and van der Vaart, A. W. (2000). Convergence rates of posterior distributions. *Ann. Statist.*, 28(2):500–531.
- [16] Ghosh, P. and Chakrabarti, A. (2017). Asymptotic optimality of one-group shrinkage priors in sparse high-dimensional problems. *Bayesian Anal.*, 12(4):1133–1161.
- [17] Ghosh, P., Tang, X., Ghosh, M., and Chakrabarti, A. (2016). Asymptotic properties of bayes risk of a general class of shrinkage priors in multiple hypothesis testing under sparsity. *Bayesian Anal.*, 11(3):753–796.
- [18] Griffin, J. E. and Brown, P. J. (2010). Inference with normal-gamma prior distributions in regression problems. *Bayesian Anal.*, 5(1):171–188.
- [19] Griffin, J. E. and Brown, P. J. (2013). Some priors for sparse regression modelling. *Bayesian Anal.*, 8(3):691–702.
- [20] Johnstone, I. M. and Silverman, B. W. (2004). Needles and straw in haystacks: Empirical bayes estimates of possibly sparse sequences. *Ann. Statist.*, 32(4):1594–1649.
- [21] Park, T. and Casella, G. (2008). The bayesian lasso. *Journal of the American Statistical Association*, 103(482):681–686.
- [22] Ročková, V. (2017). Bayesian estimation of sparse signals with a continuous spike-and-slab prior. *Ann. Statist.* To appear.
- [23] Singh, D., Febbo, P. G., Ross, K., Jackson, D. G., Manola, J., Ladd, C., Tamayo, P., Renshaw, A. A., D’Amico, A. V., Richie, J. P., Lander, E. S., Loda, M., Kantoff, P. W., Golub, T. R., and Sellers, W. R. (2002).

- Gene expression correlates of clinical prostate cancer behavior. *Cancer Cell*, 1(2):203 – 209.
- [24] Strawderman, W. E. (1971). Proper bayes minimax estimators of the multivariate normal mean. *Ann. Math. Statist.*, 42(1):385–388.
- [25] van der Pas, S., Salomond, J.-B., and Schmidt-Hieber, J. (2016). Conditions for posterior contraction in the sparse normal means problem. *Electron. J. Statist.*, 10(1):976–1000.
- [26] van der Pas, S., Szabó, B., and van der Vaart, A. (2017). Adaptive posterior contraction rates for the horseshoe. *Electron. J. Statist.*, 11(2):3196–3225.
- [27] van der Pas, S. L., Kleijn, B. J. K., and van der Vaart, A. W. (2014). The horseshoe estimator: Posterior concentration around nearly black vectors. *Electron. J. Statist.*, 8(2):2585–2618.
- [28] Wellcome Trust (2007). Genome-wide association study of 14,000 cases of seven common diseases and 3000 shared controls. *Nature*, 447:661–678.